

TIDAL AND CURRENT PREDICTION
FOR THE AMAZON'S NORTH CHANNEL
USING A HYDRODYNAMICAL-NUMERICAL MODEL

Luiz Antonio de Carvalho Ferraz

CANTLEY KNOX LIBRARY
NAVAL POSTGRADUATE SCHOOL
MONTEREY, CALIFORNIA 93940

NAVAL POSTGRADUATE SCHOOL

Monterey, California



THESIS

TIDAL AND CURRENT PREDICTION
FOR THE AMAZON'S NORTH CHANNEL
USING A HYDRODYNAMICAL-NUMERICAL MODEL

by

Luiz Antonio de Carvalho Ferraz

September 1975

Thesis Advisor:

Stevens P. Tucker

Approved for public release; distribution unlimited.

T 169/9

Unclassified

SECURITY CLASSIFICATION OF THIS PAGE (When Data Entered)

REPORT DOCUMENTATION PAGE		READ INSTRUCTIONS BEFORE COMPLETING FORM
1. REPORT NUMBER	2. GOVT ACCESSION NO.	3. RECIPIENT'S CATALOG NUMBER
4. TITLE (and Subtitle) Tidal and Current Prediction for the Amazon's North Channel Using a Hydrodynamical-Numerical Model		5. TYPE OF REPORT & PERIOD COVERED Master's Thesis; September 1975
7. AUTHOR(s) Luiz Antonio de Carvalho Ferraz		6. PERFORMING ORG. REPORT NUMBER
9. PERFORMING ORGANIZATION NAME AND ADDRESS Naval Postgraduate School Monterey, California 93940		8. CONTRACT OR GRANT NUMBER(s)
11. CONTROLLING OFFICE NAME AND ADDRESS Naval Postgraduate School Monterey, California 93940		10. PROGRAM ELEMENT, PROJECT, TASK AREA & WORK UNIT NUMBERS
14. MONITORING AGENCY NAME & ADDRESS (if different from Controlling Office) Naval Postgraduate School Monterey, California 93940		12. REPORT DATE September 1975
		13. NUMBER OF PAGES
		15. SECURITY CLASS. (of this report) Unclassified
		15a. DECLASSIFICATION/DOWNGRADING SCHEDULE
16. DISTRIBUTION STATEMENT (of this Report) Approved for public release; distribution unlimited.		
17. DISTRIBUTION STATEMENT (of the abstract entered in Block 20, if different from Report)		
18. SUPPLEMENTARY NOTES		
19. KEY WORDS (Continue on reverse side if necessary and identify by block number) Hydrodynamical-numerical model Amazon River Numerical model Tidal model Amazon's tides		
20. ABSTRACT (Continue on reverse side if necessary and identify by block number) The hydrodynamical-numerical prediction model developed by W. Hansen is applied to the North Channel of the Amazon River for computation of tides and currents; the results are compared with tidal prediction obtained by the harmonic method and to actual current measurements. A medium size grid of square mesh cells, 1800 m in length, represents the North Channel. The driving forces are the tides at the northern		

Unclassified

Unclassified

SECURITY CLASSIFICATION OF THIS PAGE(When Data Entered)

opening of the channel near the river's mouth and the river discharge into the channel at the southern end. The numerical results for tides were verified at three tidal stations, and it was observed that the tides predicted at the northern part of the channel agreed, in the worse case, within 12% of the tidal range, but those predicted at the southern end were unsatisfactorily reproduced. This fact is attributed to the size of the grid which is too coarse to describe adequately the variable and irregular cross-sections and bottom topography at the southern part of the channel. The predicted currents were in acceptable agreement with the few available measurements.

Unclassified

SECURITY CLASSIFICATION OF THIS PAGE(When Data Entered)

Tidal and Current Prediction for the Amazon's North Channel
Using a Hydrodynamical-Numerical Model.

by

Luiz Antonio de Carvalho Ferraz
Lieutenant-Commander, Brazilian Navy
B.S., United States Naval Postgraduate School, 1974.

Submitted in partial fulfillment of the
requirements for the degree of

MASTER OF SCIENCE IN OCEANOGRAPHY

170815
F2645
c.1

ABSTRACT

The hydrodynamical-numerical prediction model developed by W. Hansen is applied to the North Channel of the Amazon River for computation of tides and currents; the results are compared with tidal prediction obtained by the harmonic method and to actual current measurements. A medium size grid of square mesh cells, 1800 m in length, represents the North Channel. The driving forces are the tides at the northern opening of the channel near the river's mouth and the river discharge into the channel at the southern end. The numerical results for tides were verified at three tidal stations, and it was observed that the tides predicted at the northern part of the channel agreed, in the worse case, within 12% of the tidal range, but those predicted at the southern end were unsatisfactorily reproduced. This fact is attributed to the size of the grid which is too coarse to describe adequately the variable and irregular cross-sections and bottom topography at the southern part of the channel. The predicted currents were in acceptable agreement with the few available measurements.

TABLE OF CONTENTS

I.	INTRODUCTION-----	13
A.	REVIEW-----	13
B.	OBJECTIVE-----	14
II.	DESCRIPTION OF THE NORTH CHANNEL OF THE AMAZON RIVER-----	16
A.	GENERAL-----	16
B.	CHARACTERISTICS OF THE TIDES AND CURRENTS IN THE AMAZON RIVER-----	17
C.	THE AREA OF STUDY-----	18
III.	THE HANSEN HYDRODYNAMICAL MODEL-----	21
A.	ASSUMPTIONS AND BASIC EQUATIONS-----	21
B.	FINITE DIFFERENCE EQUATIONS-----	23
C.	GRID SELECTION-----	28
D.	INPUT OF TIDES AND RIVER DISCHARGE-----	29
E.	TUNING THE MODEL-----	34
F.	MODEL-----	34
IV.	DISCUSSION-----	58
V.	SUMMARY-----	63
	APPENDIX A: NUMERICAL PROGRAMS-----	64
	BIBLIOGRAPHY-----	81
	INITIAL DISTRIBUTION LIST-----	83

LIST OF TABLES

I.	Compilation of Some Discharge Measurements and Investigations in the Amazon River and Estuary-----	32
II.	Current Velocity and Direction Predicted at the Three Tide Stations by the HN-Model-----	37
III.	Computer Output for Water Elevation and Resultant Current Velocity and Direction in 12 Selected Locations-----	54

LIST OF FIGURES

1.	North Channel of the Amazon-----	19
2.	Grid Net Scheme-----	24
3.	Grid Net Laid over the North Channel of the Amazon-----	30
4.	Amazon River Cross-Section near Macapa, Looking Downstream-----	33
5.	Tuning the Model-----	35
6.	Current Velocity at the Three Tide Stations-----	38
7.	(a) Currents in the North Channel after 75 Hours-----	41
	(b) Currents in the North Channel after 76 Hours-----	41
8.	(a) Currents in the North Channel after 77 Hours-----	42
	(b) Currents in the North Channel after 78 Hours-----	42
9.	(a) Currents in the North Channel after 79 Hours-----	43
	(b) Currents in the North Channel after 80 Hours-----	43
10.	(a) Currents in the North Channel after 81 Hours-----	44
	(b) Currents in the North Channel after 82 Hours-----	44
11.	(a) Currents in the North Channel after 83 Hours-----	45
	(b) Currents in the North Channel after 84 Hours-----	45
12.	(a) Currents in the North Channel after 85 Hours-----	46
	(b) Currents in the North Channel after 86 Hours-----	46
13.	(a) Currents in the North Channel after 87 Hours-----	47
	(b) Currents in the North Channel after 88 Hours-----	47
14.	(a) Currents in the North Channel after 89 Hours-----	48
	(b) Currents in the North Channel after 90 Hours-----	48
15.	(a) Currents in the North Channel after 91 Hours-----	49
	(b) Currents in the North Channel after 92 Hours-----	49

16. (a) Currents in the North Channel after 93 Hours-----	50
(b) Currents in the North Channel after 94 Hours-----	50
17. (a) Currents in the North Channel after 95 Hours-----	51
(b) Currents in the North Channel after 96 Hours-----	51
18. (a) Currents in the North Channel after 97 Hours-----	52
(b) Currents in the North Channel after 98 Hours-----	52
19. Currents in the North Channel after 99 Hours-----	53
20. Prediction of Tides at Limao do Curua-----	55
21. Prediction of Tides at Acaituba-----	56
22. Prediction of Tides at Macapa-----	57

TABLE OF SYMBOLS AND ABBREVIATIONS

cm	centimeter
cm ²	square centimeter
cm ³	cubic centimeter
cm/sec	centimeter per second
cm ² /sec	cubic centimeter per second
d	total difference
F	friction force
f	Coriolis parameter
g	acceleration of gravity
H	total depth ($H = h + \zeta$)
h	depth of water at mean water level
HM	harmonic method of prediction of tides
HN	hydrodynamical-numerical prediction model
hr	hour
HTU, HTV	depth at U- and V- grid points
HT	high tide
HTZ	symbolic depth at Z-grid points
K	coefficient of horizontal kinematic eddy viscosity
km	kilometer
km ²	square kilometer
L	characteristic length
ℓ	length of the mesh
LT	low tide
M, N or m, n	grid coordinates

m	meter
m ²	square meter
m ³	cubic meter
m ³ /sec	cubic meter per second
n mile	nautical mile
NE, ME	grid delimiters
NEH, MEH	near border grid coordinates (NEH = NE - 1, MEH = ME - 1)
p	hydrostatic pressure
R	bottom roughness coefficient
r	coefficient of bottom friction
t	time
u, v	velocity components
U, V	mean u and v components
\vec{V}	total velocity vector
$W_{(x)}, W_{(y)}$	wind speed components
X, Y or x, y	space coordinates
Z, U, V	grid points
α	smoothing parameter
β	1 - α
δ	partial difference
γ	specific weight
λ	drag coefficient
ζ	water level anomaly
ρ	density of the fluid
τ	wind stress
τ^b	bottom stress

$\vec{\omega}$	earth angular velocity
Δ	difference, also, in figures, represents tide station
Δt	half-time step
∇^2	$\frac{\delta^2}{\delta x^2} + \frac{\delta^2}{\delta y^2}$ (Laplacian)

ACKNOWLEDGEMENT

I wish to express my sincere thanks to everyone who has assisted in the preparation of this study, in particular to the personnel of the Department of Oceanography of the Environmental Prediction Research Facility, especially to Dr. Taivo Laevastu, Mr. Kevin Rabe, and Mr. Arthur D. Stroud. Finally to Dr. Stevens P. Tucker, my thesis advisor, my gratitude for his patience, understanding, translation of German references and bibliography and for his constant constructive criticism that greatly contributed to the completion of this project.

I. INTRODUCTION

A. REVIEW

Pressure gradients are the dominant mechanisms in rivers, narrow estuaries and some lakes which are opposed by friction [21]. In large scale circulation the opposing forces are combinations of friction and the Coriolis force or the latter alone.

Hydraulic models have been used for many years to reproduce the physical characteristics of rivers and have proven to be reliable, but space and operating problems make them a relatively expensive tool of investigation. The appearance of high speed computers made possible the numerical solution of the differential equations used to describe flow. A physical model can be transformed into a program which may be modified easily to simulate different conditions and may be stored for future utilization and alteration, thus allowing solutions to be obtained rapidly and at a reasonable cost.

The hydrodynamical-numerical method developed by W. Hansen makes it possible to determine the motion in oceanic areas, in adjacent and marginal seas, in shelf areas as well as in estuaries and rivers [15, 18]. In many cases the method has been applied successfully to the quantitative reproduction of tides and storm surges. The numerical treatment of the hydrodynamical equations requires the bathymetry, boundary geometry, and meteorological and density structure to be considered.

This model has been applied to rivers such as the Eider, the Ems and the Elbe, in Germany [9, 17, 18]. The Eider is a tidal river in northern Germany with very irregular cross-sections and a remarkably irregular depth distribution. Application of the HN-model with a very fine mesh, to approximate the cross-sections by a number of parallel canals of differing width and depth, produced good results with a maximum deviation of 30 cm between computed and observed tides, which is less than 10% of the tidal range. Later computations with improvements in the longitudinal direction from grid point to grid point made it possible to reduce the deviations between the computed and observed values to below 3.5 cm, which was about 1% of the tidal range [17]. Similar applications of the HN-model were made to the Ems and the Elbe, and the results were in all cases of the same order of magnitude. For the Elbe the differences were smaller than 2 cm [9, 17].

In this study the hydrodynamical-numerical prediction model of Hansen is applied to the Amazon's North Channel and the results are compared to field observations.

B. OBJECTIVE

The objective of this thesis is to predict by means of the Hansen hydrodynamical-numerical model tides and currents which exist in the North Channel of the Amazon River during an intermediate river stage and to compare the numerical results with available field measurements. The computed tides are compared to prediction by harmonic method at three tide stations along the channel and the currents are compared to field observations at selected locations.

A medium size square mesh grid is used to represent the North Channel's configuration and bottom topography. The numerical results will provide means of evaluating this representation in terms of grid size as well as of the merits and limitations of the HN-model.

II. DESCRIPTION OF THE NORTH CHANNEL OF THE AMAZON RIVER

A. GENERAL

The Amazon River is located in South America, where it begins its eastward flow from a chain of glacier-fed lakes in the Andes Mountains in central Peru. It emerges from the eastern foothills of the Andes, sweeps through the world's largest tropical rain forest, and discharges into the Atlantic Ocean on the northern coast of Brazil. En route to the Atlantic the river drains about 7×10^6 km² of land, receiving the flow of over 200 tributaries.

The Amazon is the world's largest river in terms of drainage area and discharge. Its discharge is subjected to seasonal fluctuations. Two periods are generally considered: (1) that from April to June, the rain season or the high water stage; and (2) that from October to December, the season of low precipitation or low water stage.

Investigations and measurements made by the University of Brazil, the Brazilian Navy, and the U.S. Geological Survey in 1963 and 1964 produced some astonishing numbers for the flow of the river. The flow at Obidos (some 850 km from the mouth) during the high stage measured about 216,000 m³/sec, during low stage about 72,500 m³/sec, and during an intermediate stage, 164,520 m³/sec. The average flow, estimated for the discharge into the Atlantic Ocean, was slightly over 175,000 m³/sec [2, 19, 20].

The river is generally deep, and in more than ten locations depths greater than 100 m have been found. The width of the

channel ranges from about 2 km at its narrowest up to about 10 km in some places, with long sections having intermediate values [2, 19].

Gibbs [12] and Diegues [3] have shown that the Amazon waters spread over the Atlantic Ocean in a variable layer, 10 to 20 m thick, under which the oceanic water progresses towards the shore. Gibbs [12] showed that during the high stage of the river a vertical stratification ranges out over the continental shelf, to distances of 80 to 230 km from the mouth, and during the low stage it ranges out to 60 to 185 km. However, all vertical isohalines indicative of turbulent mixing are limited to the mouth of the river, and there is never penetration of salt water into the river as occurs in some types of estuaries [12, 13].

B. CHARACTERISTICS OF THE TIDES AND CURRENTS IN THE AMAZON RIVER

The Amazon River seems to have the longest river tide-zone in the world [1]. Tides are observed up to the vicinity of Santarem harbor, some 800 km from the river's mouth, but during extremely low flows tidal effects have reached upstream to Obidos. The tides are of semidiurnal type with a maximum range of about 5 m. Field measurements indicate that the tidal variation decreases upstream.

Tides and river flow combine to produce strong currents in many sites upstream. The North Channel (Fig. 1) has a single main entrance from the sea, but numerous small tributaries and channels also offer secondary connections to the ocean.

In many of these channels a tidal bore is a peculiar characteristic.

Franco [8] characterizes the current in the North Channel in the vicinity of Macapa as "alternating-axial" (rectilinear or reversing), that is, the alternating current component superimposed on the main downstream river flow is maximum upstream during the high water, maximum downstream during the low water and it is zero when the tide is at the mean water level. There is a relatively strong permanent current downstream due to the enormous discharge of the river.

C. THE AREA OF STUDY

The Amazon discharges into the Atlantic in two branches. The present study is limited to a region of the upper branch which constitutes the North Channel, extending some 147 km from the mouth. This channel is the navigable waterway from the river's mouth to the ports of Macapa and Santana in the Brazilian Federal Territory of Amapa (Fig. 1).

The Port of Santana is utilized mainly by the large vessels that carry manganese ore extracted from the mines of Serra do Navio, inland of Amapa. Navigation in the North Channel is somewhat difficult due to natural conditions in the river, such as enormous floating trees, sometimes attached to floating grass "islands," pulled down from the adjacent margins by erosion, strong currents, and a large tidal variation. The harbor at Santana is of the floating type to compensate for the large tidal range and for the seasonal fluctuations of the river level. The port of Macapa consists mainly of a wharf where

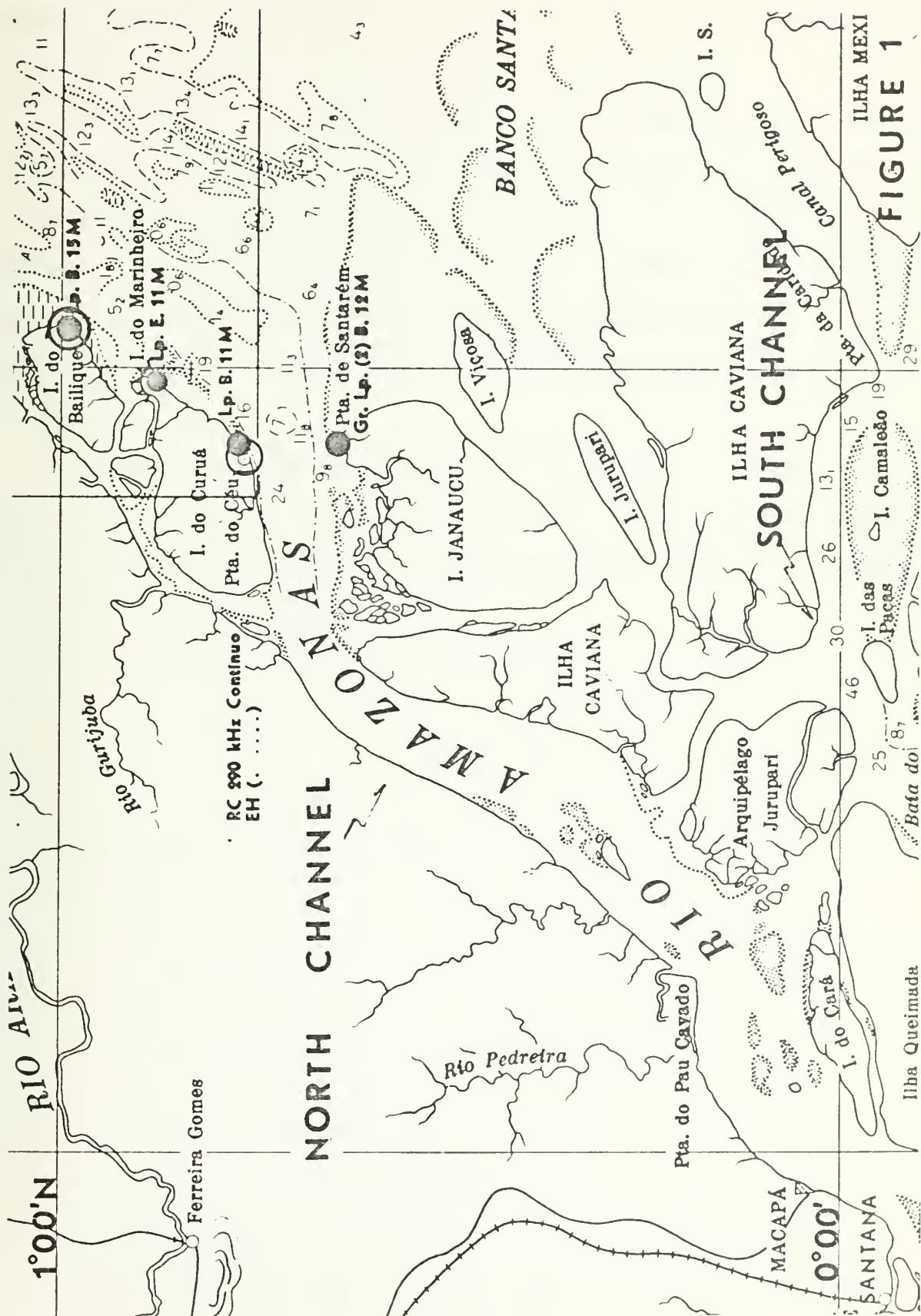


FIGURE 1

small vessels and typical river boats load and unload passengers and light cargoes.

The Channel is generally oriented in a SW-NE direction, has an average depth of 20 m and is never narrower than 5.5 km. In some places, as in the vicinity of Macapa, the configuration of the river bed is quite variable, with irregular cross-sections and bottom topography. The bottom is composed mainly of mud and sand, and the banks and bars along the river are also of these materials.

A tidal bore does not manifest itself in the North Channel, but in the shallow sites near the mouth of the small tributaries and channels discharging into the main river bores are of very common occurrence.

III. THE HANSEN HYDRODYNAMICAL MODEL

A. ASSUMPTIONS AND BASIC EQUATIONS

The assumptions leading to a Hansen-type hydrodynamical model are the following:

1. The fluid is homogeneous and incompressible;
2. Pressure is hydrostatic, and thus the changes in pressure are due solely to changes in water surface elevation;
3. Advection terms are neglectable;
4. The fluid is in hydrostatic equilibrium in the vertical direction; and
5. The geographical and vertical variations of the Coriolis force may be neglected.

The basic equations for the single layer hydrodynamical model developed by Hansen follow from the application of these assumptions to the equations of conservation of momentum. Reference [10] presents the derivation of the equations.

Horizontal momentum equations are integrated over depth to give:

$$\frac{\delta U}{\delta t} - fV = -g \frac{\delta \zeta}{\delta x} + K \nabla^2 U - \frac{\tau^b(x)}{H} + \frac{\tau(x)}{H} + X \quad (1)$$

$$\frac{\delta V}{\delta t} + fU = -g \frac{\delta \zeta}{\delta y} + K \nabla^2 V - \frac{\tau^b(y)}{H} + \frac{\tau(y)}{H} + Y \quad (2)$$

$$\frac{\delta \zeta}{\delta t} + \frac{\delta}{\delta x}(HU) + \frac{\delta}{\delta y}(HV) = 0 \quad (3)$$

The wind stress components are represented by:

$$\tau_{(x)} = \lambda W_x [W_x^2 + W_y^2]^{1/2} \quad (4)$$

$$\tau_{(y)} = \lambda W_y [W_x^2 + W_y^2]^{1/2} \quad (5)$$

The bottom stress components are given by:

$$\tau^b_{(x)} = r U [U^2 + V^2]^{1/2} \quad (6)$$

$$\tau^b_{(y)} = r V [U^2 + V^2]^{1/2} \quad (7)$$

The various terms in the above equations being defined as:

K = coefficient of horizontal kinematic eddy viscosity

λ = drag coefficient

W_x, W_y = wind speed components

ζ = surface elevation

H = total depth ($H = h + \zeta$)

g = acceleration of gravity

f = Coriolis parameter

x, y = space coordinates

X, Y = components of external forces

U, V = water velocity components

$$(U = \frac{1}{H} \int_{-h}^{\zeta} u dz, V = \frac{1}{H} \int_{-h}^{\zeta} v dz)$$

r = bottom friction coefficient

$$\nabla = \frac{\delta}{\delta x} + \frac{\delta}{\delta y}$$

The equations for bottom friction and wind stress are empirically developed. The wind stress terms as used in the model are assumed to be quadratic expressions in wind velocity, where λ is the wind drag coefficient with a typical value of

3.2×10^{-6} [6, 7, 10]. The bottom stress is assumed to be nonlinearly dependent on U and V, and like the wind stress it was derived by empirical means. It was originally formulated for a shallow water application and the use of this value for deep water is questionable, since it probably should be smaller in such an application. The value of r for this particular case was recommended by Laevastu (personal communication) as 2.8×10^{-3} to 3.0×10^{-3} .

B. FINITE DIFFERENCE EQUATIONS

The differential equations are solved by a "leapfrog" or central-difference scheme for time dependent solutions. At the boundaries the values of the velocity components and surface elevation are taken at actual points rather than from the surrounding points as shown in Fig. 2.

The driving forces are the tides at the open boundaries and the wind at the surface over the entire field. The tidal values are computed at each time step and introduced as new values of ζ at each point on the boundary.

The finite-difference form of the equations is given below. Using the equation of conservation of mass, the water elevation is first calculated:

$$\begin{aligned} \zeta^{t+\tau}(n,m) = & \bar{\zeta}^{t-\tau}(n,m) - \frac{\tau}{\Delta} [H_u^t(n,m) U^t(n,m) - H_u^t(n,m-1) U^t(n,m-1) \\ & + H_v^t(n-1,m) V^t(n-1,m) - H_v^t(n,m) V^t(n,m)] \end{aligned} \quad (8)$$

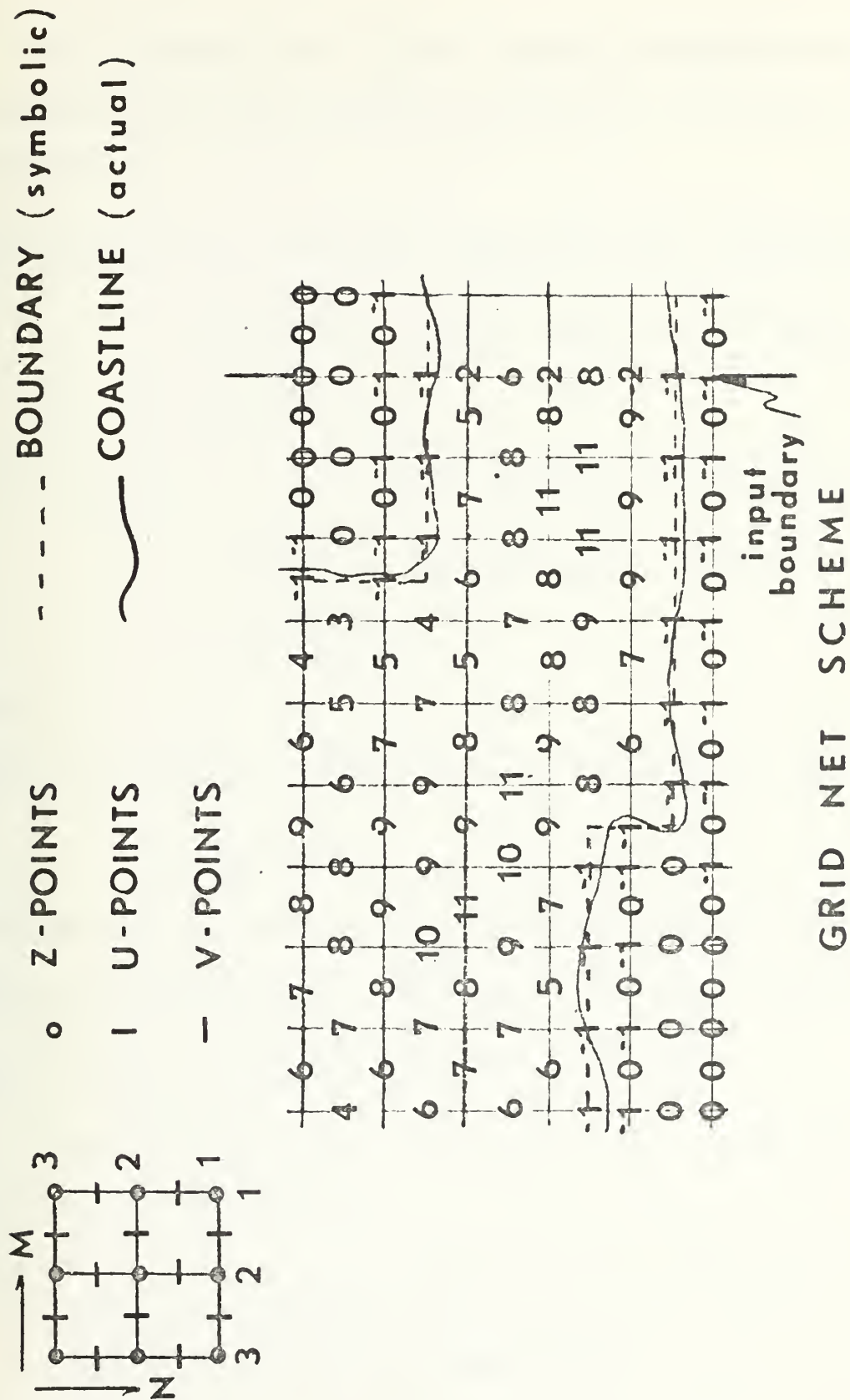


FIGURE 2

The horizontal and vertical velocity components are then determined from the respective horizontal and vertical momentum equations:

$$\begin{aligned}
 U^{t+2\tau}(n,m) = & [1 - (2\tau r / H_u^{t+2\tau}(n,m)) (\bar{U}^t(n,m)^2 + \bar{V}^{*t}(n,m)^2)^{1/2} \bar{U}^t(n,m)] \\
 & + 2\tau f \bar{V}^{*t}(n,m) - \frac{\tau g}{\ell} [\zeta^{t+\tau}(n,m+1) - \zeta^{t+\tau}(n,m)] \\
 & + 2\tau X^{t+2\tau}(n,m)
 \end{aligned} \tag{9}$$

$$\begin{aligned}
 V^{t+2\tau}(n,m) = & [1 - (2\tau r / H_v^{t+2\tau}(n,m)) (\bar{V}^t(n,m)^2 + \bar{U}^{*t}(n,m)^2)^{1/2} \bar{V}^t(n,m)] \\
 & - 2\tau f \bar{U}^{*t}(n,m) - \frac{\tau g}{\ell} [\zeta^{t+\tau}(n,m) - \zeta^{t+\tau}(n+1,m)] \\
 & + 2\tau Y^{t+2\tau}(n,m)
 \end{aligned} \tag{10}$$

where:

$$\begin{aligned}
 \bar{U}^t(n,m) = & \alpha U^t(n,m) + \frac{1-\alpha}{4} [U^t(n-1,m) + U^t(n+1,m) + U^t(n,m+1) \\
 & + U^t(n,m-1)]
 \end{aligned} \tag{11}$$

$\bar{V}^t(n,m)$ and $\zeta^t(n,m)$ have expressions analogous to $\bar{U}^t(n,m)$,

$$\bar{U}^{*t}(n,m) = \frac{1}{4} [U^t(n,m-1) + U^t(n+1,m-1) + U^t(n,m) + U^t(n+1,m)],$$

and $\bar{V}^{*t}(n,m)$ is similarly analogous to $\bar{U}^{*t}(n,m)$. (12)

The time step is 2τ . The total depth H_u or H_v at u- or v-points is computed as:

$$H_u^{t+2\tau}(\text{or } v)(n,m) = h_u(n,m) + \frac{1}{2} [\zeta^{t+\tau}(n,m) + \zeta^{t+\tau}(n,m+1)] \tag{13}$$

The effects of wind are computed by:

$$x^t = \frac{\lambda}{H} W_x^t [(W_x^t)^2 + (W_y^t)^2]^{1/2} - \frac{1}{\rho} \frac{\delta P}{\delta x} \circ \quad (14)$$

$$y_t = \frac{\lambda}{H} W_y^t [(W_x^t)^2 + (W_y^t)^2]^{1/2} - \frac{1}{\rho} \frac{\delta P}{\delta y} \circ \quad (15)$$

where P_o is the barometric pressure. It is assumed that the pressure gradient is zero for small areas and normal conditions.

The stability of the finite-difference scheme is governed by the Courant-Friedrich-Levy criterion which states that the maximum length of the time step is determined by the grid size, ℓ , and maximum depth, H_{\max} :

$$\Delta t = \frac{\ell}{\sqrt{2gH_{\max}}} \quad (16)$$

For this particular grid, a value of 30 seconds was used for the one-half time step, Δt .

When the computational area contains small regions of great depth, a "false-bottom" can be used in these sections [7]. For example, areas deeper than 500 m may be assumed to be 500 m deep. This will often result in a considerable increase in time step or a decrease in the grid length if total computation time is a critical factor. Experimental results have shown that the errors introduced with this procedure are acceptable in some cases for practical applications of the model.

The grid net is formed by three different sets of points as shown in Fig. 2, the water elevation (Z-points) and the two components of the velocity (U- and V-points). Each of these points has the same coordinate designation (N,M).

The coastline must pass through the U- and V-points and never through the Z-points. The program reads the values of the depth at U- and V-points as HTU and HTV, respectively.

The Z-points are for water, land and coast designation, being read by the program as HTZ. They are treated symbolically as 1, 0 and -1 respectively. The HTU and HTV show the chart depth in centimeters, while the coastline is symbolized by -1 and the land by 0, depending on their location in the grid. At the open boundaries the points HTZ have symbolic values of -2 and -3 for the first and second boundary when applicable. Outside these boundaries, values of 0 for HTZ are prescribed.

The coefficient of horizontal kinematic eddy viscosity is related to the values of the U and V components. Hansen states that the computations are always stable for values of $\beta = (1 - \alpha)$ between 0 and 0.5. This coefficient can also be used as a tuning factor: the higher the value, the smoother the current velocity distribution. In areas where the depth distribution is irregular, as in this case, accelerations and surface irregularities appear in the model. These abnormalities can be corrected for by means of a proper smoothing of the bottom or of the water surface elevation; in this model this is accomplished by smoothing the water surface elevation, which is a numerical artifact of the model.

In finite-difference form, the coefficient of horizontal kinematic eddy viscosity is given by the relation:

$$K = \frac{\Delta \ell^2 (1 - \alpha)}{4 \Delta t}$$

For this model with a value of alpha equal to 0.983 recommended by Laevastu (personal communication), K becomes 0.46×10^{-5} cm²/sec..

High values of alpha must be used with caution, because these can allow undesirable oscillations in the model. Also, if too low a value is used to provide higher smoothing, the current velocity may be overly damped.

As was pointed out in the assumptions of the Hansen model, the mean advective terms, $u_j \delta u_i / \delta x_j$, have been neglected. This is not necessarily a good assumption as these terms can be the same order of magnitude as the local acceleration terms, $\delta u_i / \delta t$. In the derivation of the time averaged equations of motion, the turbulent contribution of the advective terms, as expressed by the Reynold's stresses, have been included using the linearizing eddy diffusivity approximation. Hence, the non-linear effects are not included but the amplitude effects of the advective terms are included by the eddy diffusivity approximation.

C. GRID SELECTION

The grid size is selected upon requirements of detail and accuracy and the availability of computer core memory and time. There is not a general rule for selection of the grid mesh, but for open areas and round smooth bays, where the expected values of current velocity and direction fields are smooth, a fine mesh is not necessary, but for areas where the topography is of primary importance, or in narrow channels, a fine mesh may be required for reliable results.

For this particular model, a medium size grid was initially considered satisfactory (see discussion on page 61 below). Decreasing the size of the mesh will result in an increase of time and computer memory. A 24 x 65 unit array of square mesh cells having sides 1800 m in length was laid over the North Channel of the Amazon River as it is represented in the Brazilian Nautical Chart No. 220 (BRASIL - RIO AMAZONAS, carta 220 "Da Barra Norte ao Porto de Santana," DHN - Rio de Janeiro).

Experiments performed at the Environmental Prediction Research Facility (EPRF) have proven that there is not much increase in accuracy for smaller grid size; for example, a model for the San Diego Bay was run under three different meshes, and except in computation of advection and dispersion of pollutants, no significant differences were recorded between fine and coarse grids.

D. INPUT OF TIDES AND RIVER DISCHARGE

The tides in this model were inputed at the northern opening in the grid which was chosen and oriented such that the closest tidal station in that location lay over or near a grid-point, along the $M = 2$ grid line. This tidal entrance is parallel to the y- coordinate.

The tides at the station LIMA DO CURUA (Fig. 3) were introduced with seven components, M_2 , S_2 , N_2 , K_2 , L_2 , K_1 and MS_4 . Two other tide stations provide means of comparison for the tides predicted by the HN-model: ACAITUBA and MACAPA, 58 km and 142 km upstream, respectively. Usually only four components are introduced in the model, but the values of the

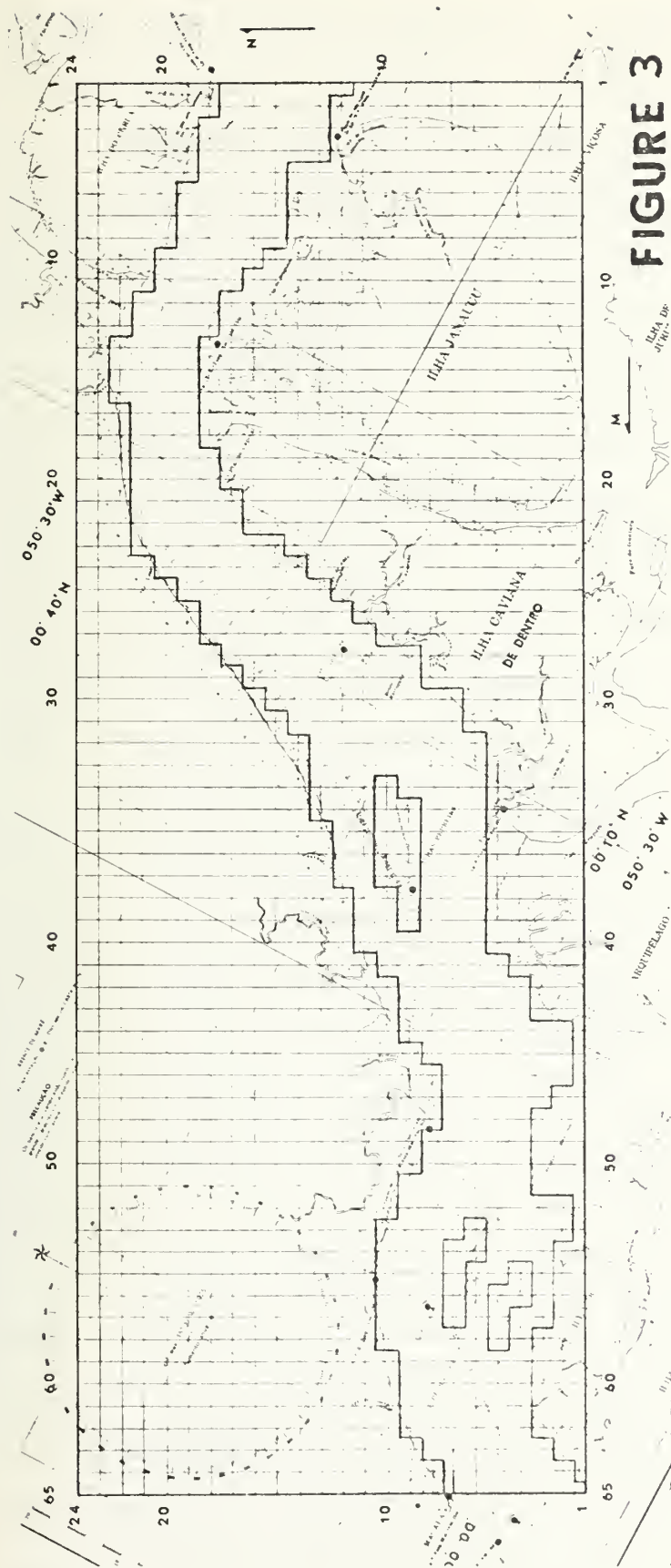


FIGURE 3

GRID-NET OVER THE AMAZON'S NORTH CHANNEL, AS IT IS REPRESENTED IN THE BRAZILIAN NAUTICAL CHART NO. 220. THE ARROWS LABELED "N" AND "M" INDICATE THE DIRECTION OF INCREASING N AND M GRID-COORDINATES.

seven constituents introduced in this particular case were considered quite significant.

The river discharge was inputed as permanent current, averaged from the bottom to the surface, in a cross-section near Macapa along the y-grid line at the southern end of the grid. This input boundary was left open to insure continuity.

There is no adequate measurement of the river discharge in the North Channel at the present time. There are, however, some estimates and calculations of the river discharge at Macapa and at the mouth and some current measurements made by the Brazilian Navy for navigation purposes. Table I shows a compilation of the more recent investigations and measurements for the Amazon's discharge.

The flow of the Amazon is seasonal and can be correlated with precipitation in the entire Amazon region. Diegues [3] states that during the year the variation of the level of the river is quite sufficient, the water level being closely related to precipitation in the Amazon Basin to a large degree and the melting of snow in the Andes Mountains to a small degree. Such variations are periodic and follow a yearly cycle.

The value used for this model is an estimated averaged value for Macapa, $175,000 \text{ m}^3/\text{sec}$, and it is most generally accepted. Such value which is expected to represent the mean or intermediate stage for the river was distributed over the cross-section in Macapa, as shown in Fig. 4, to produce the mean velocities (permanent downstream flow) to be inputed in grid points, in a manner similar to that described by Dronkers [4].

Date	Location	River Stage	Width m	Area m ²	Mean Velocity m/sec	Discharge m ³ /sec	Source
7-16-63	Obidos	High	2,290	110,000	1.97	216,000	Oltman, 1968
11-20-63	Obidos	Low	2,260	92,400	0.79	72,500	Oltman, 1968
8- 9-64	Obidos	Mean	2,280	106,000	1.55	165,000	Oltman, 1968
7-20-63	Manaus	High	2,097	85,654	1.74	169,104	Souza et al, 1964
7-22-63	Manaus	High	683	14,864	1.35	-	Souza et al, 1964
1967	Mouth ¹	Low	12,500	270,000	0.30	83,500	Gibbs, 1972
1967	Mouth ¹	High	12,500	310,000	0.90	267,400	Gibbs, 1972
1963	Macapa ²	High	11,204	186,218	1.14	212,378	Souza et al, 1964
1963	Mouth ²	Mean	-	-	-	175,000	Oltman, 1968
¹ At the isohaline of 20%							
² Estimative							

TABLE I - Compilation of some discharge measurements and investigations in the Amazon River and Estuary.

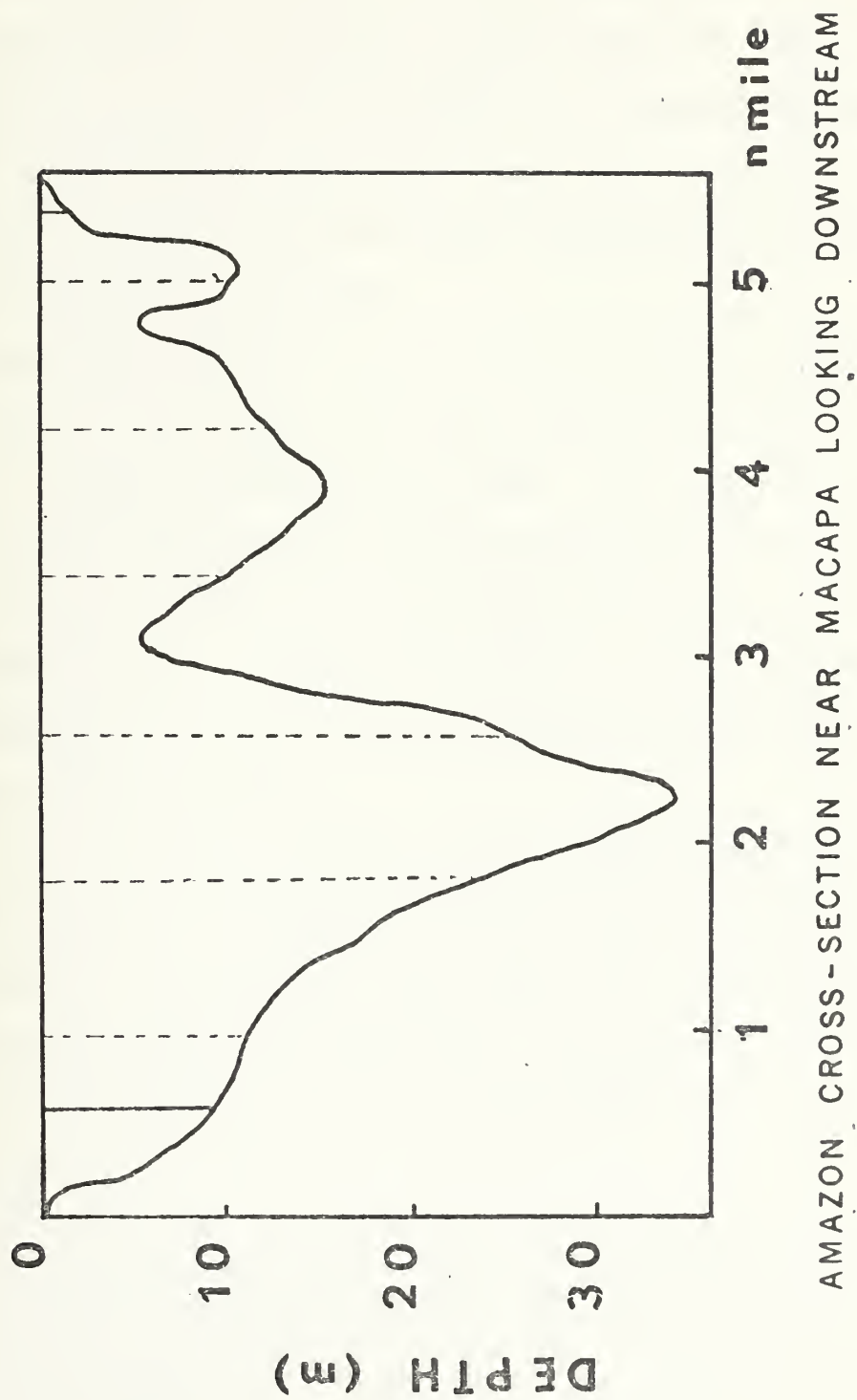


FIGURE 4

E. TUNING THE MODEL

Tuning the model is a matter of patience. Several runs of the program were made with different combinations of alpha and the bottom friction parameter. After each run both the water elevation and currents were compared to harmonic method and current measurements available. The model is left to run for some hours of real time with these combinations of parameters until stability is attained.

In general, the model appears to be rather insensitive to variations in the bottom friction coefficient, but it responds quickly to small variations in alpha. The behavior of the tidal curve at the same location for two different values of alpha ($\alpha = 0.980$, $\alpha = 0.975$) and two different values of bottom friction parameter ($r = 0.0028$, $r = 0.0030$), is illustrated in Fig. 5. When changing alpha the bottom friction parameter was maintained constant and vice-versa.

Due to a lack of adequate current measurements in the North Channel the model was mainly adjusted for the tides, and the velocities of the currents were considered satisfactory when the tide agreement was reached and the currents approached the values and directions of the few available observations.

F. MODEL

The calculated currents behave as described by Franco [8], that is, they are what is termed "alternating-axial" or sometimes "rectilinear" or "reversing." The maximum downstream velocities appear at low tide (LT) and they are greater at the first LT than in the second. Similarly, maximum upstream

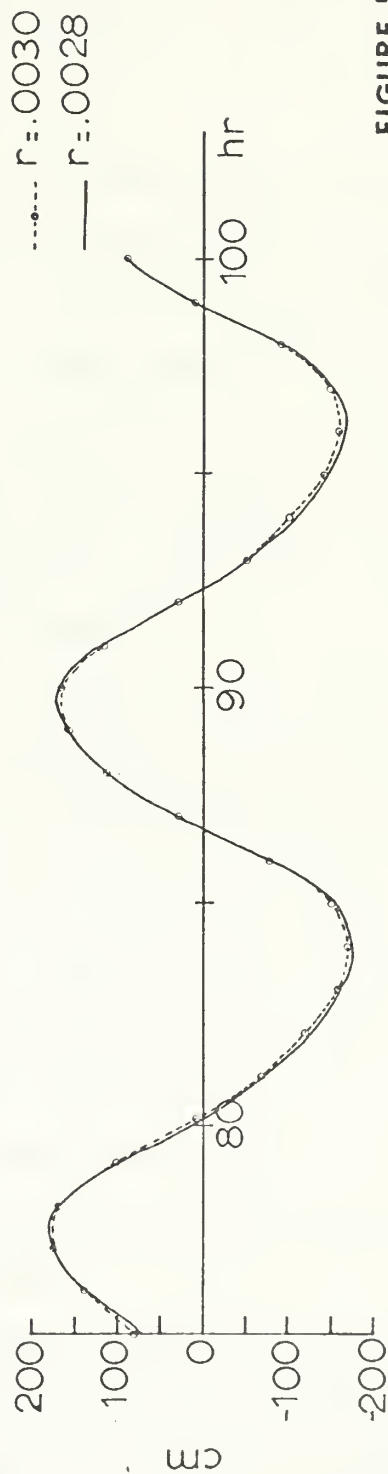
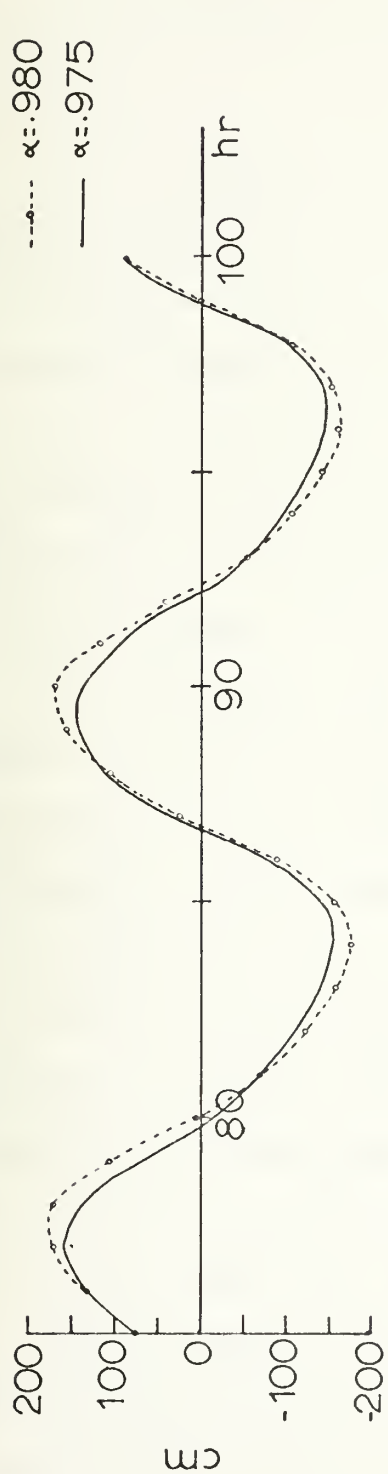


FIGURE 5

TUNING THE MODEL: ABOVE, ALPHA IS CHANGED AND THE FRICTION COEFFICIENT, r , IS MAINTAINED CONSTANT; BELOW, ALPHA IS CONSTANT AND r IS CHANGED.

velocities occur at the high tide (HT). Slack water corresponds to the crossings of the mean level.

At the grid points representing the tidal stations, the respective maximum and minimum predicted values of current were as follows:

(1) At Limao do Curua, grid coordinates (17,2), 196 cm/sec and 183 cm/sec for the first and second LT and 162 cm/sec and 157 cm/sec for the first and second HT. The direction changed from 062° (downstream) to 242° (upstream).

(2) At Acaituba, grid coordinates (11,26), 115 cm/sec and 107 cm/sec for the first and second LT and 90 cm/sec and 87 cm/sec for the first and second HT. The direction changed from 032° (downstream) to 210° (upstream).

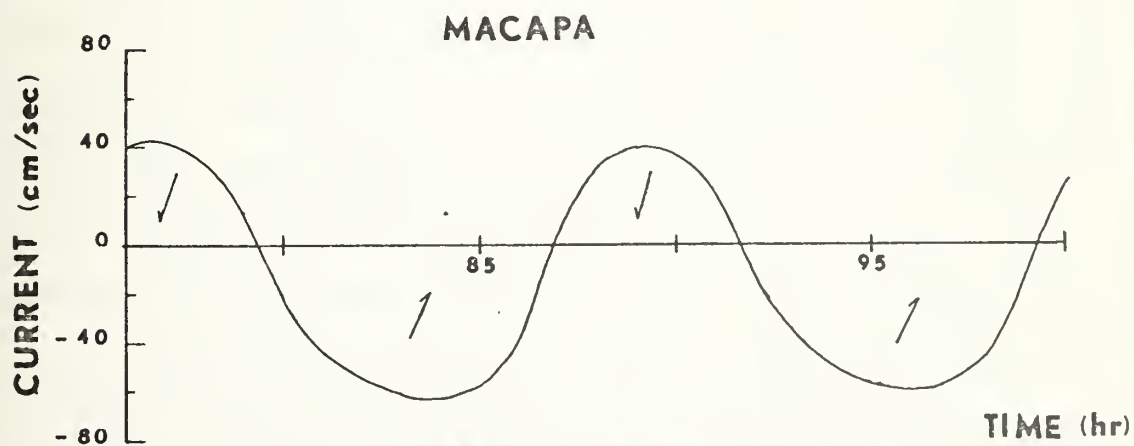
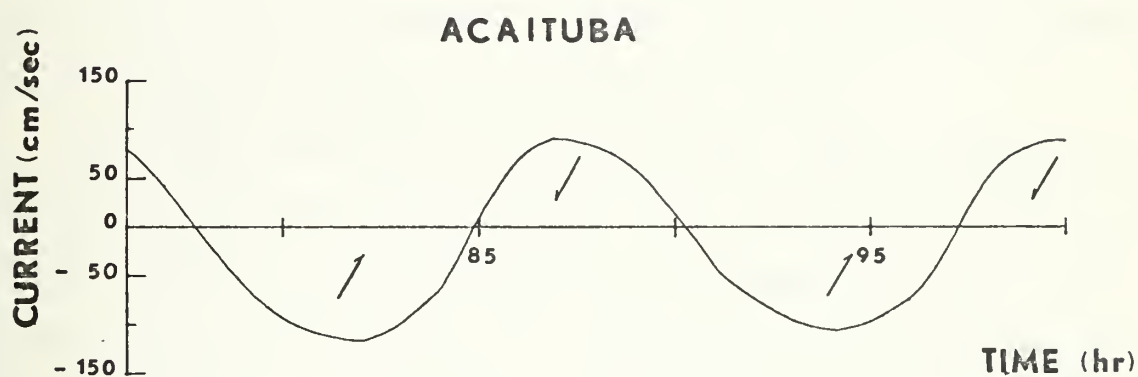
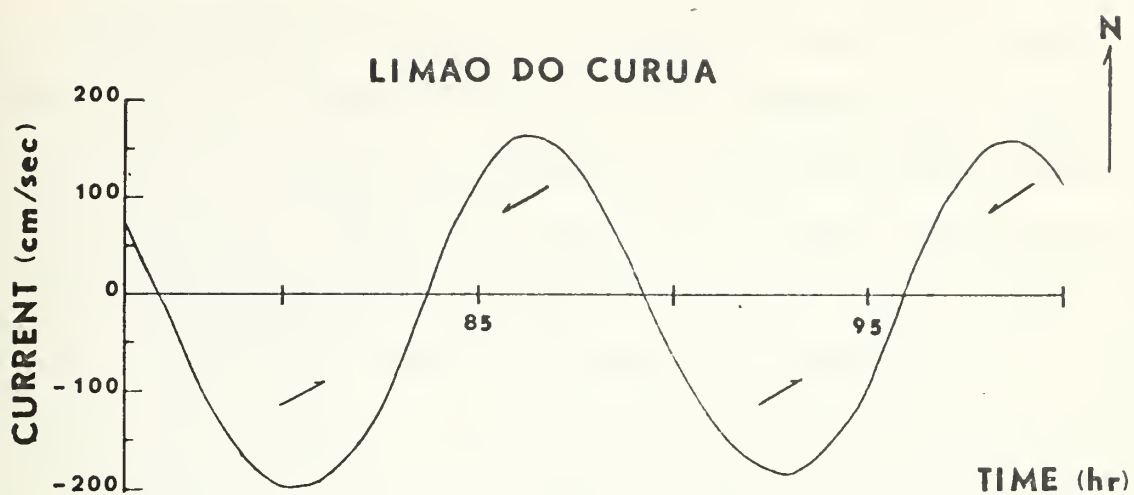
(3) At Macapa, grid coordinates (7,63), 62 cm/sec and 60 cm/sec for the first and second LT and 42 cm/sec and 40 cm/sec for the first and second HT. The direction changed from 024° (upstream) to 201° (downstream).

At these locations a phase lag of about 40 minutes between the instant of the high tide and low tide and the peak of the current is observed, but it is possible that this lag may be smaller, since the output of one hour interval of the program did not allow a precise determination of the exact instant of the low and high tide (Table II).

Figure 6 shows a plot of the current velocities at the three mentioned tide stations for the last 24 hours for a simulated 100 hours (real time) run of the program.

TIME	LIMAO DO CURUA			ACAITUBA			MACAPA		
hr	VEL cm/sec	DIR <u>o</u>		VEL cm/sec	DIR <u>o</u>		VEL cm/sec	DIR <u>o</u>	
76	73	242		80	210		40	196	◁ HT
77	11	062		43	211		42	220	
78	100	061		11	027		33	206	
79	165	062		60	031		13	202	
80	196	062	◁ LT	91	031		21	029	
81	192	063		109	032		43	026	
82	151	061		115	032	◁ LT	54	025	
83	75	062		103	032		60	024	◁ LT
84	29	242		65	033		62	024	
85	121	242		12	203		58	024	
86	162	242	◁ HT	71	209	◁ HT	41	024	
87	150	240		90	209		5	174	
88	98	242		84	210		32	194	
89	25	242		58	210		40	201	◁ HT
90	60	061		13	213		36	206	
91	132	062		41	030		21	200	
92	174	060	◁ LT	76	031		9	049	
93	183	062		97	031		35	029	
94	158	062		107	032	◁ LT	49	027	
95	98	062		103	032		56	026	◁ LT
96	6	060		76	032		60	026	
97	93	240		16	037		58	026	
98	151	242	◁ HT	56	209		47	027	
99	157	242		86	209		12	043	
100	118	242		87	210		25	194	

TABLE II - Current velocity and direction predicted by the HN-model at the three tidal stations. The left-hand column indicates the last 24 hrs of a 100-hr (real time) computer run. The right-hand columns indicate the approximate time of the low tides (LT) and high tides (HT).



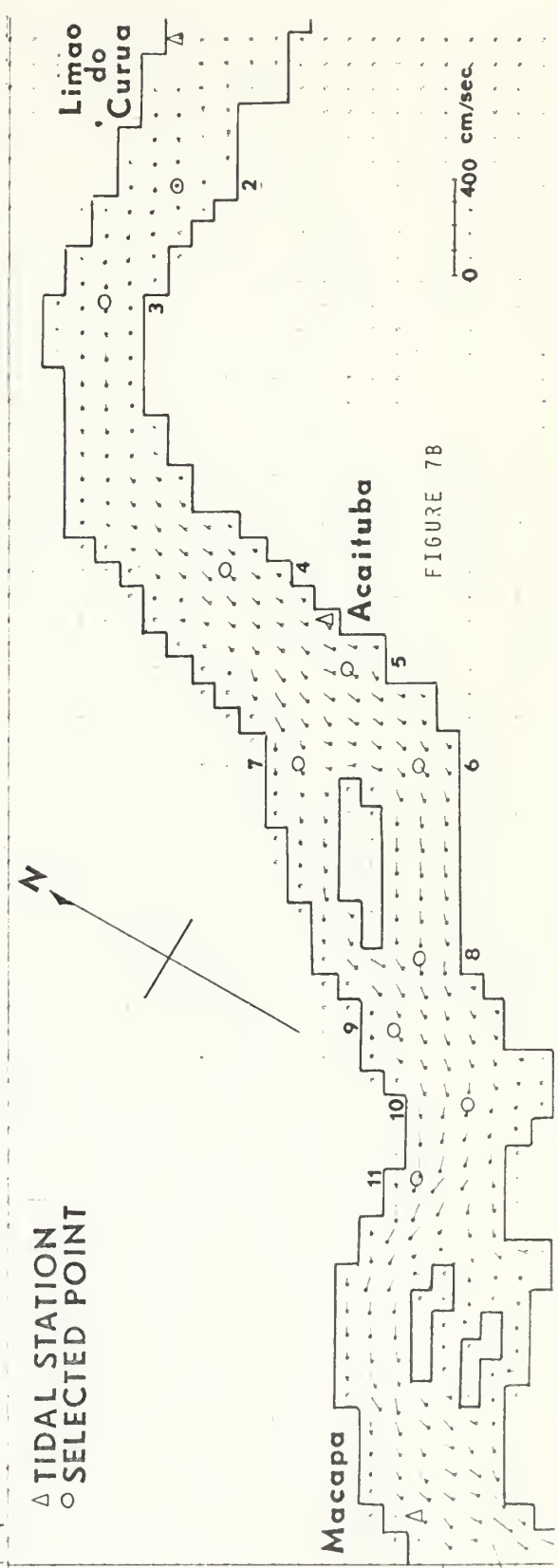
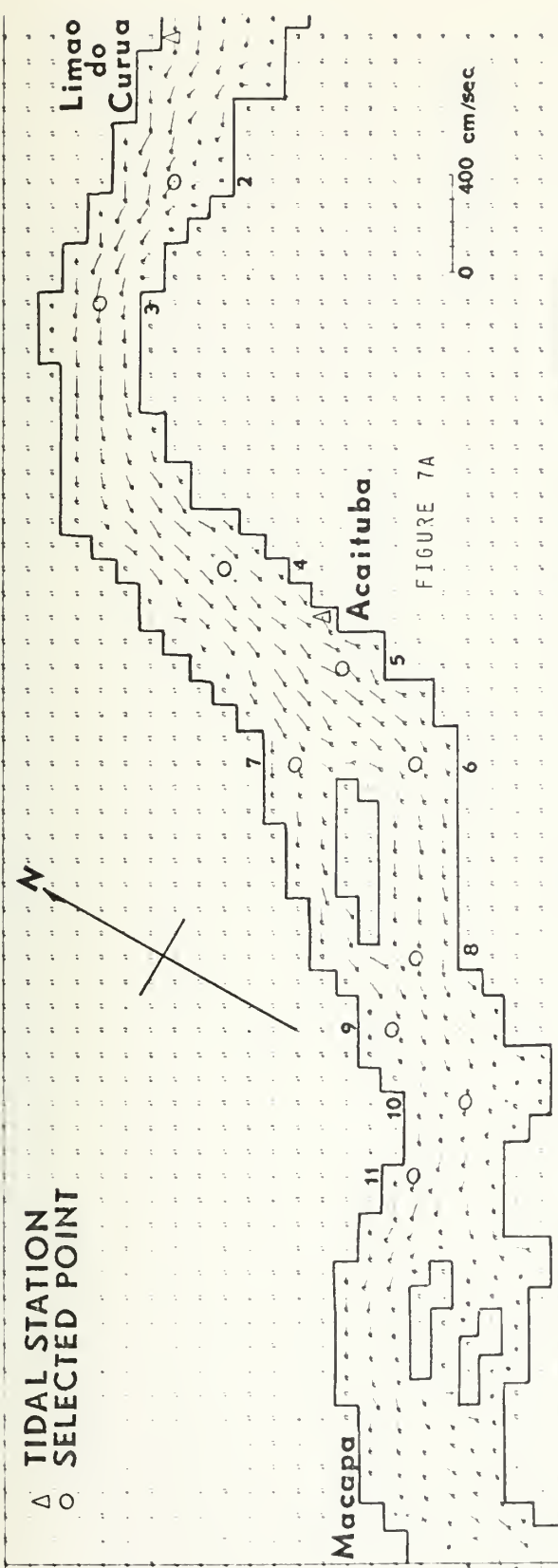
CURRENT AT TIDAL STATIONS

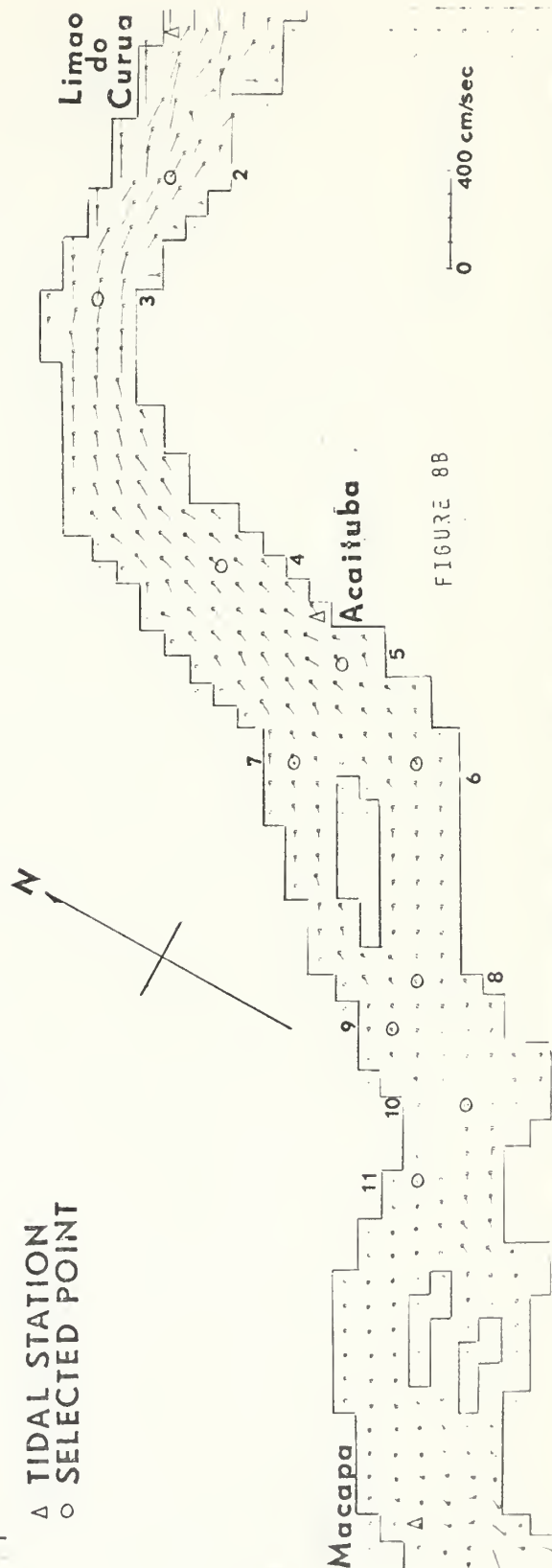
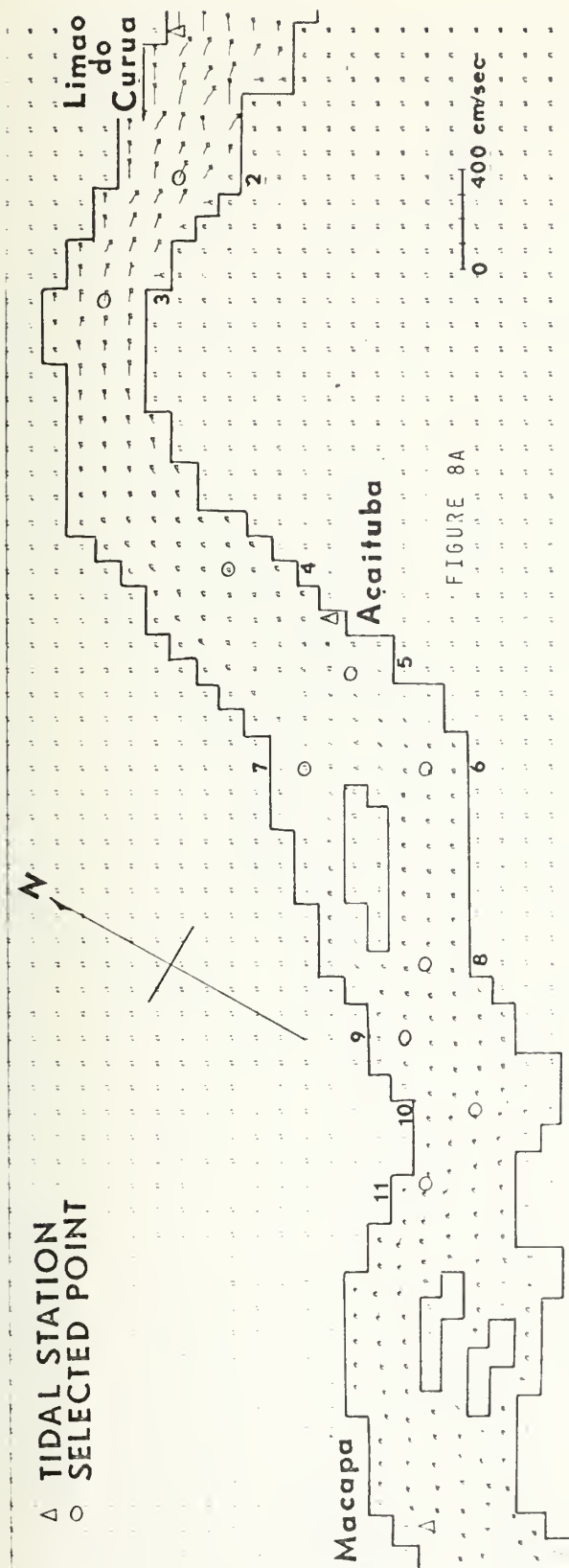
FIGURE 6

Plots of the currents in the North Channel are shown in Figs. 7 (a,b) through 19 in which the currents are scaled so that 1 cm corresponds to 157 cm/sec and the arrows indicate the directions. The full lines on the graphs represent the symbolic boundaries, the triangles represent the location of the tidal stations, and the ellipses the location of selected points. (It should be noted that the plotting subroutines used for these plots are not included in the program of Appendix A.) The water elevation and the resultant current velocity at the selected points are shown in Table III, which is a reproduction of the computer output for the special points.

The tides predicted by the model are shown in Figs. 20 through 22 for the last 24 hours of a simulated 100 hours (real time) period. In these figures is included the difference between the prediction by the numerical model (HN) and the prediction by harmonic method (HM). For Limao do Curua (Fig. 20) the maximum difference was 19 cm which represents 4% of the tidal range and a phase lag of less than 30 minutes is observed only at the first LT. For Acaituba (Fig. 21) the maximum difference was 41 cm which represents 11.7% of the tidal range but a phase lag of about 20 minutes is observed between the HN and HM prediction. This can be partially explained by the fact that the actual tide station lies in much shallower water than the closest grid point chosen to represent it and also because the distance from this grid point to the station is about 2 km.

For Macapa (Fig. 20) the results were not satisfactory. An attempt to improve the results, by smoothing the bottom, resulted in the curve labeled HN1 in the figure, but further attempts were abandoned because they would not be realistic with the actual mesh size.





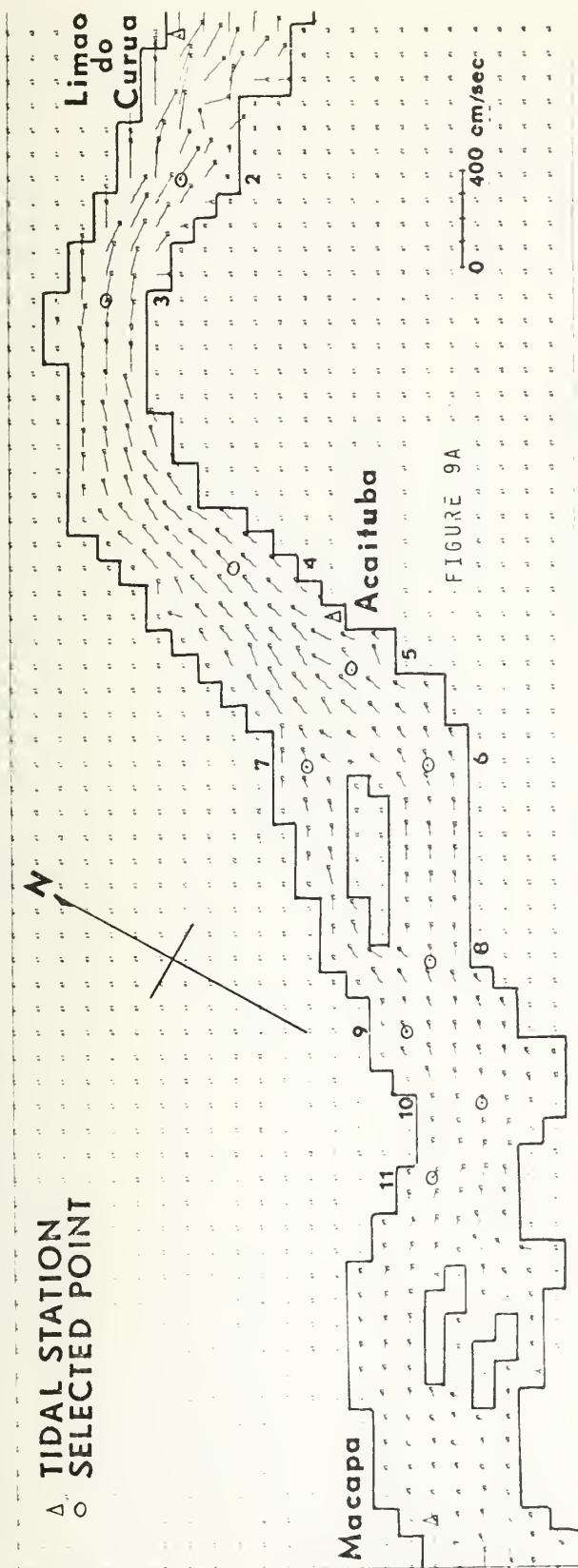


FIGURE 9A

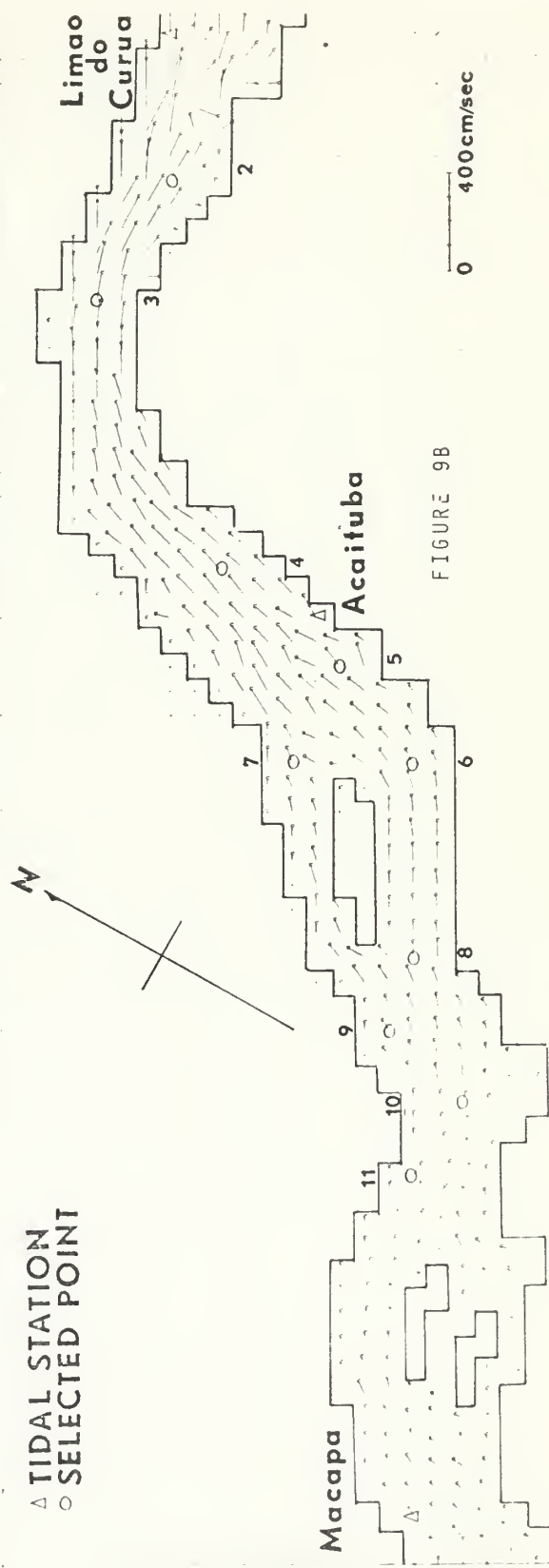
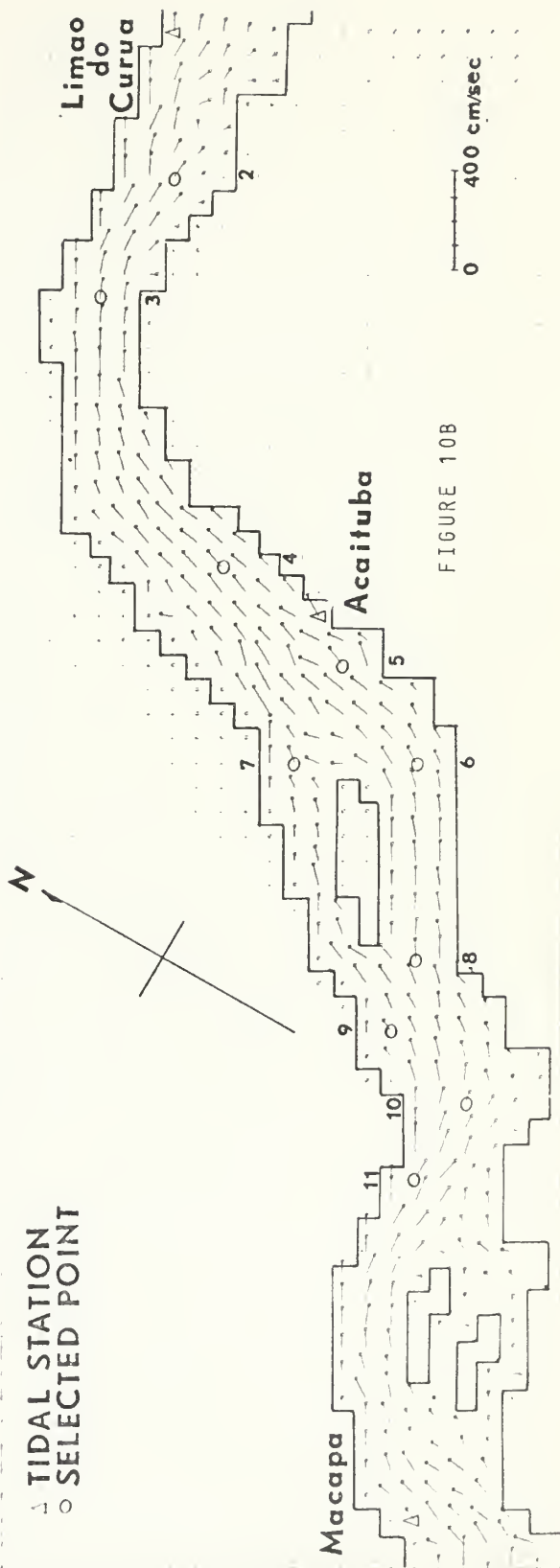
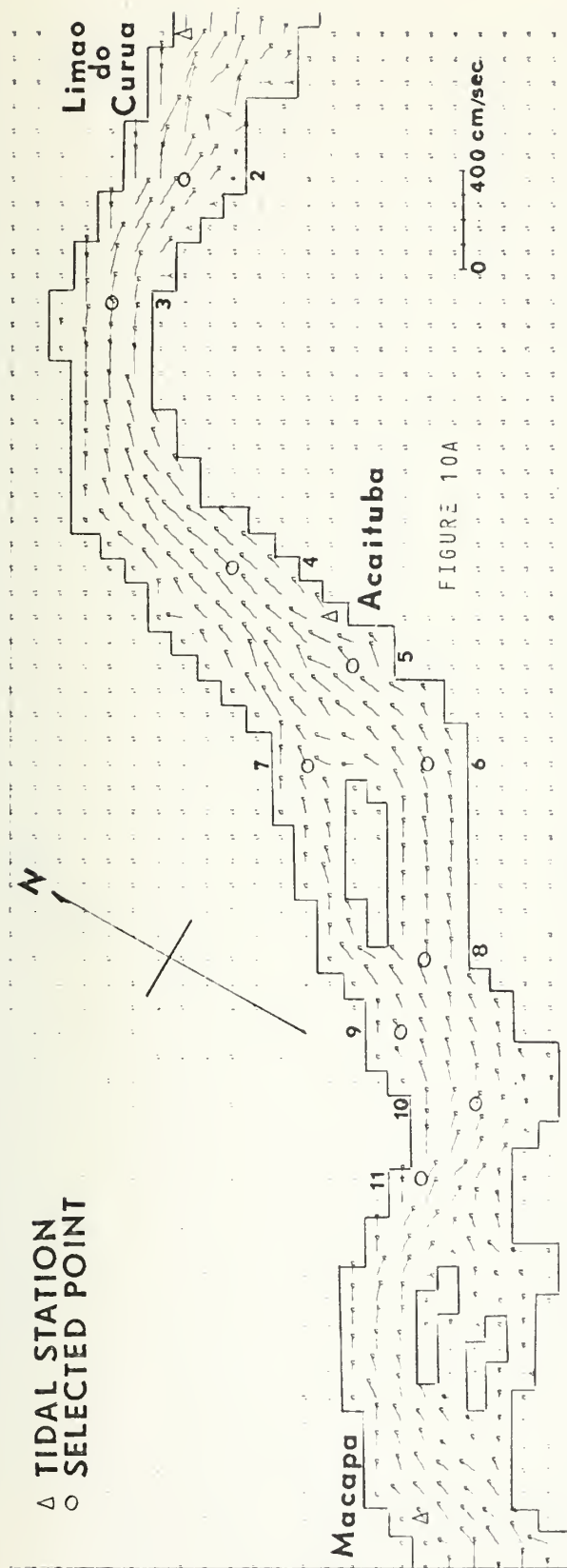
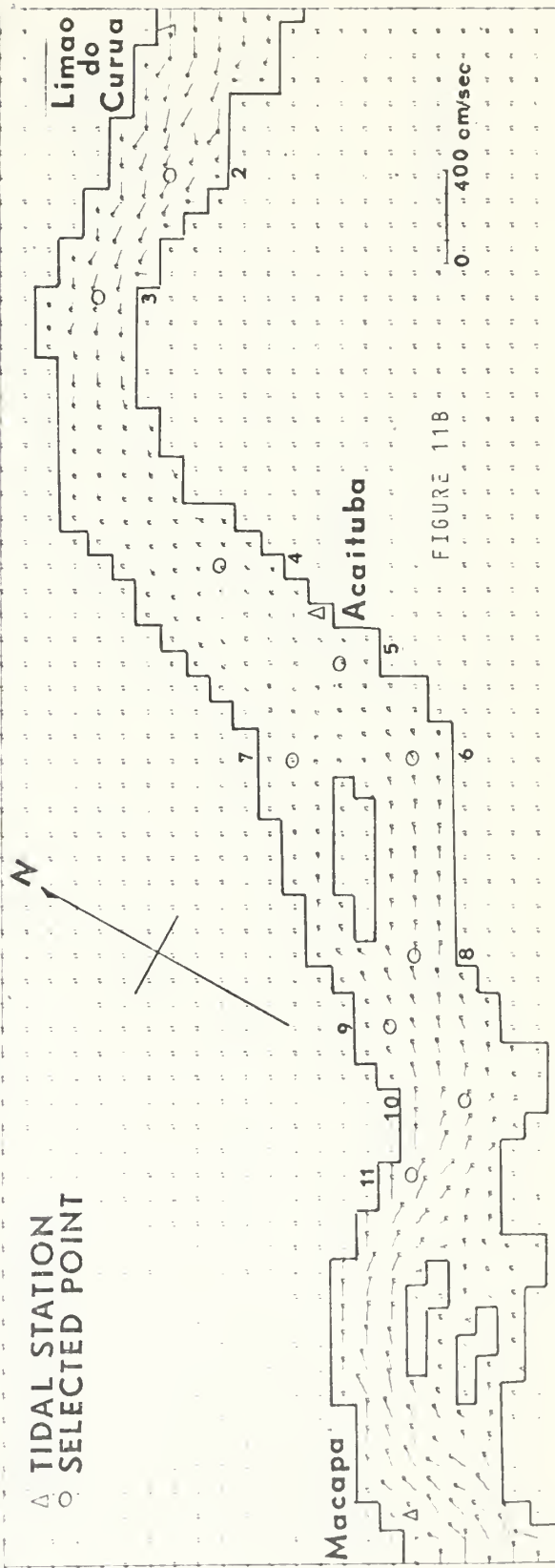
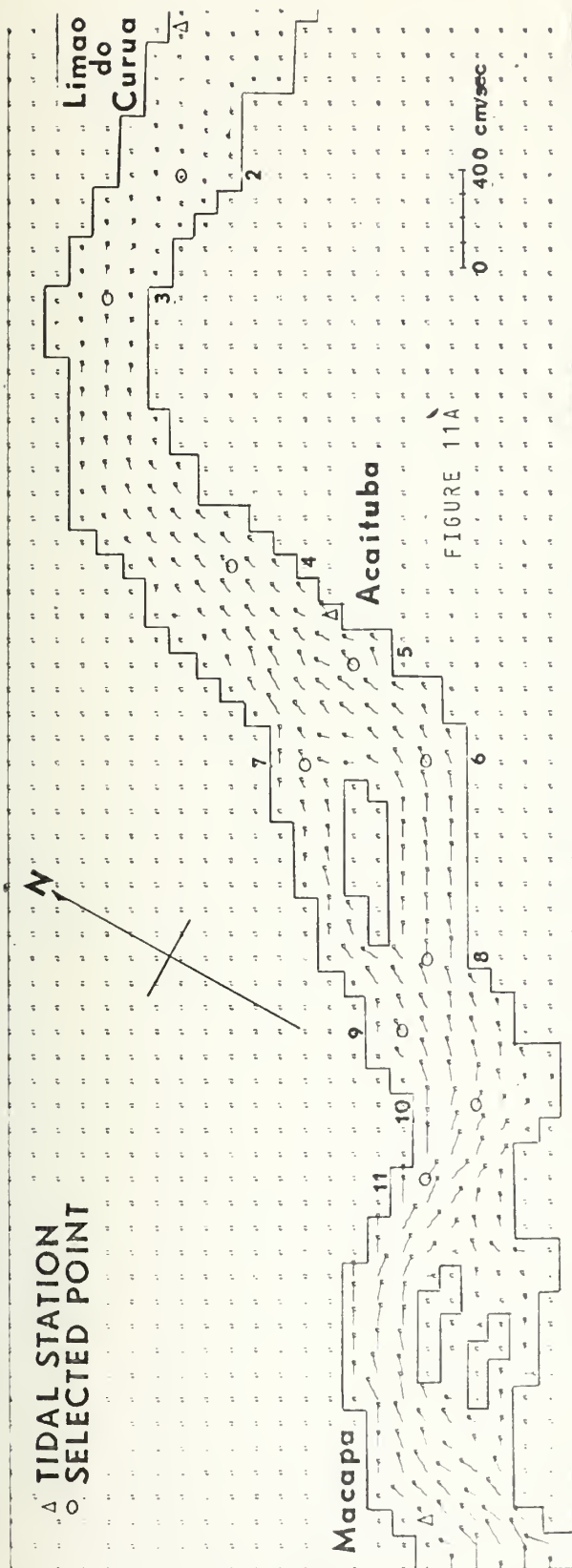


FIGURE 9B





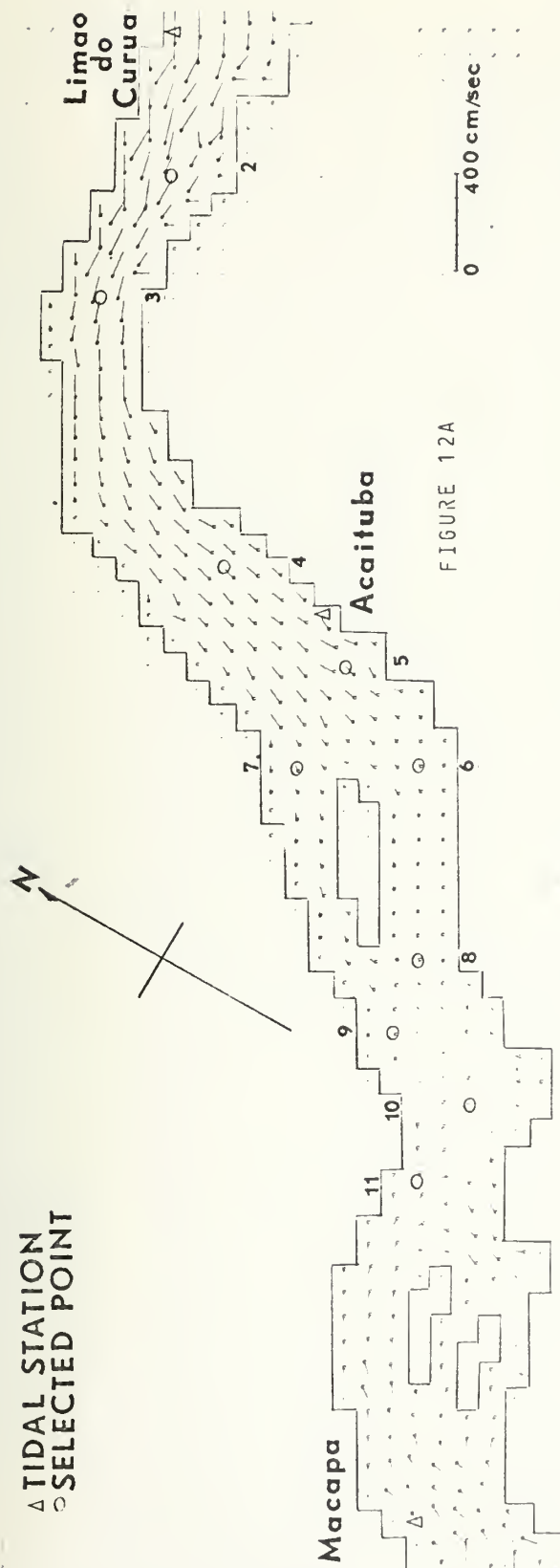


FIGURE 12A

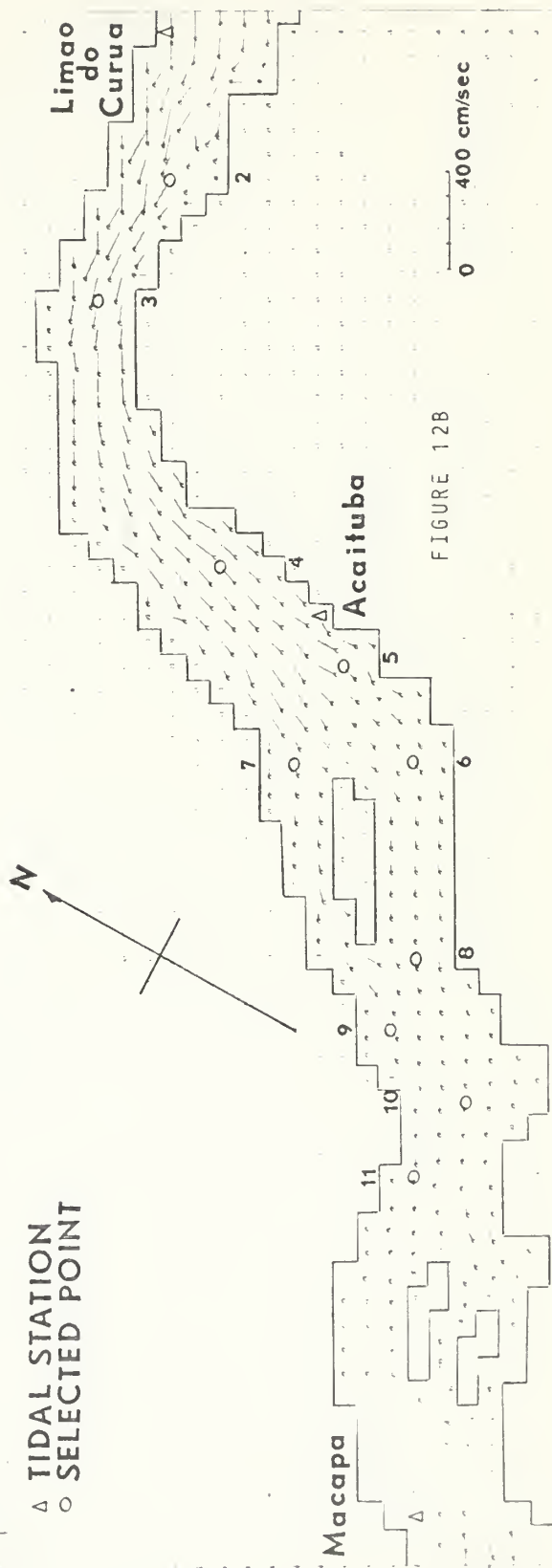
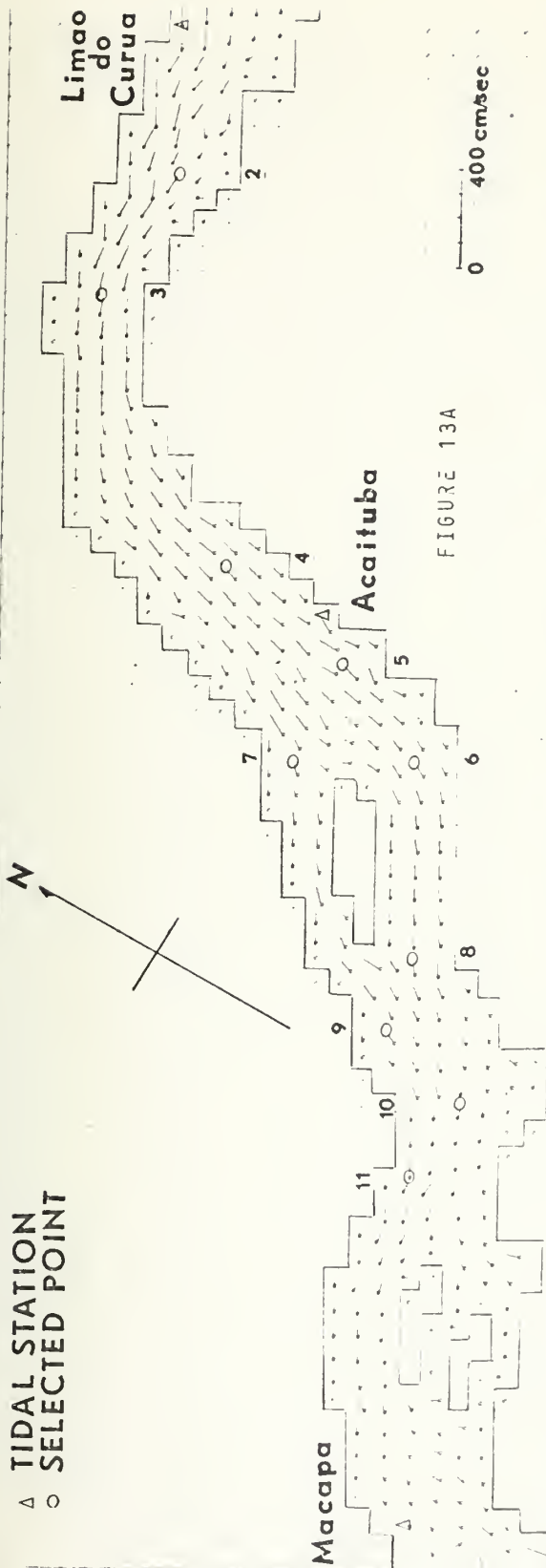
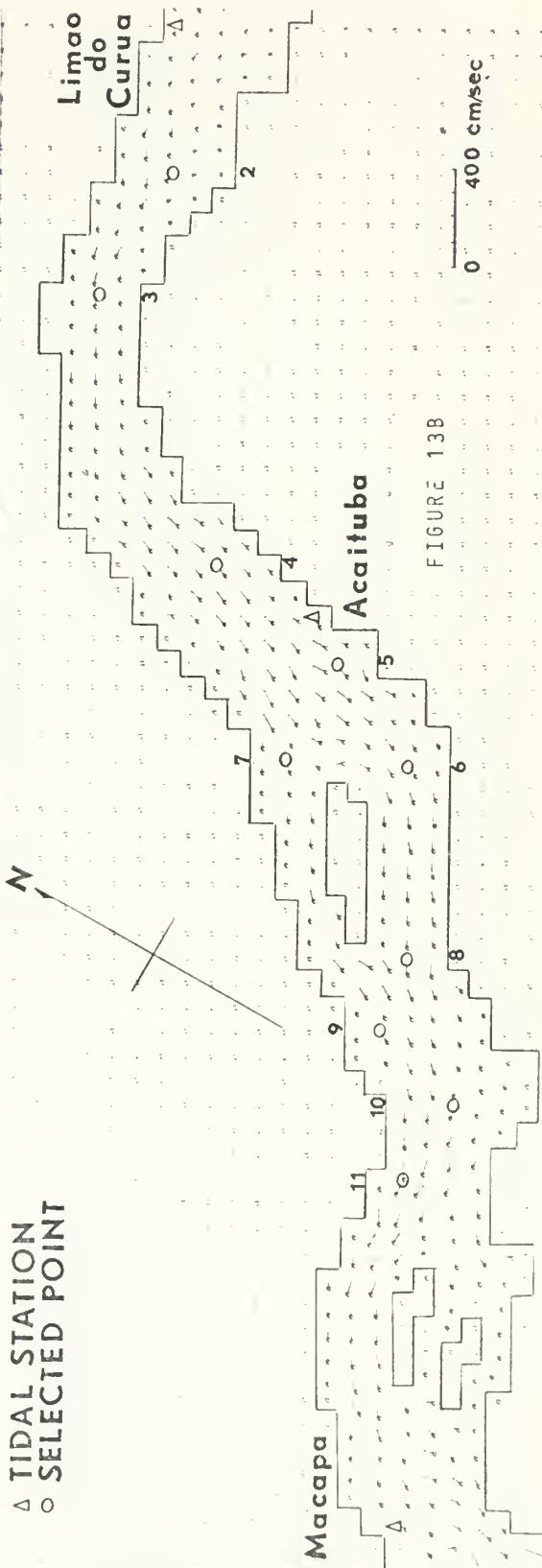


FIGURE 12B

Δ TIDAL STATION
 ○ SELECTED POINT



Δ TIDAL STATION
 ○ SELECTED POINT



Δ TIDAL STATION
○ SELECTED POINT

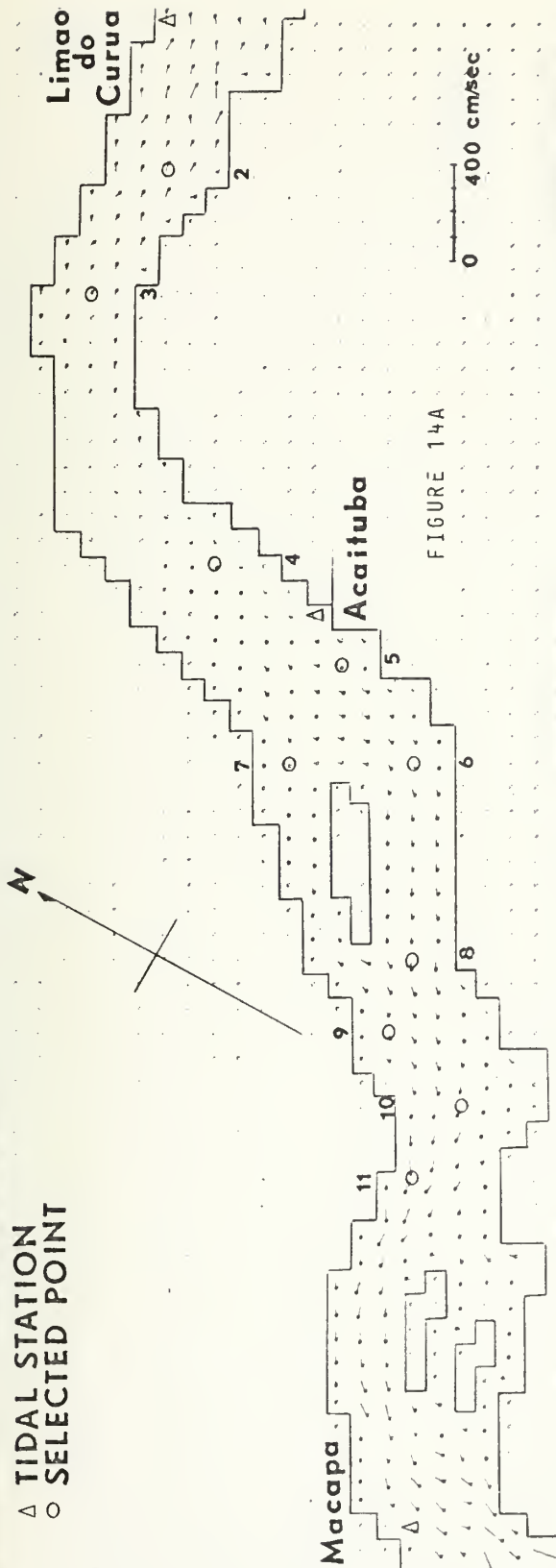


FIGURE 14A

Δ TIDAL STATION
○ SELECTED POINT

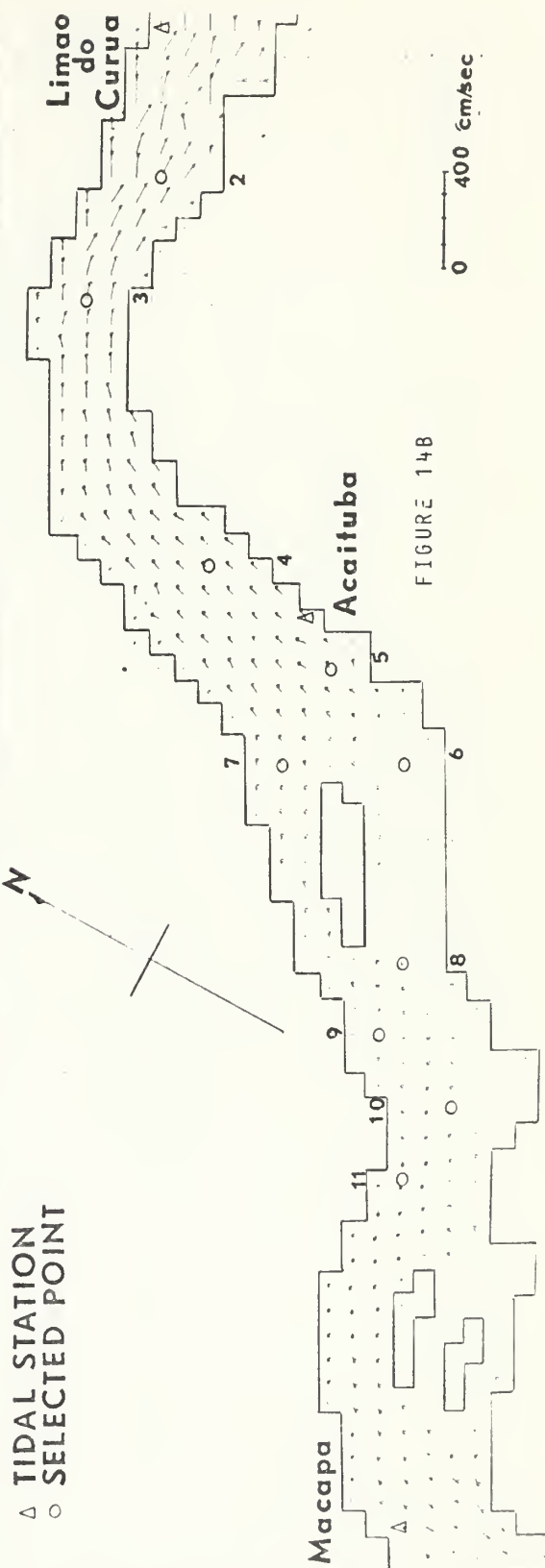


FIGURE 14B

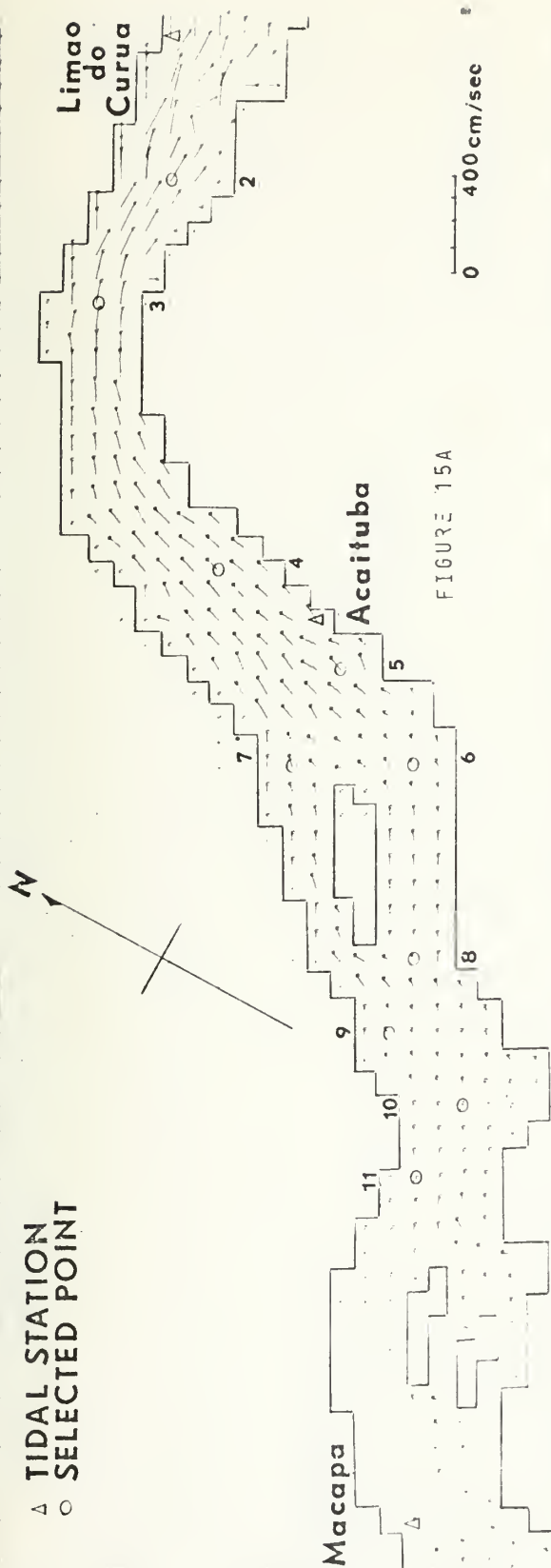


FIGURE 15A

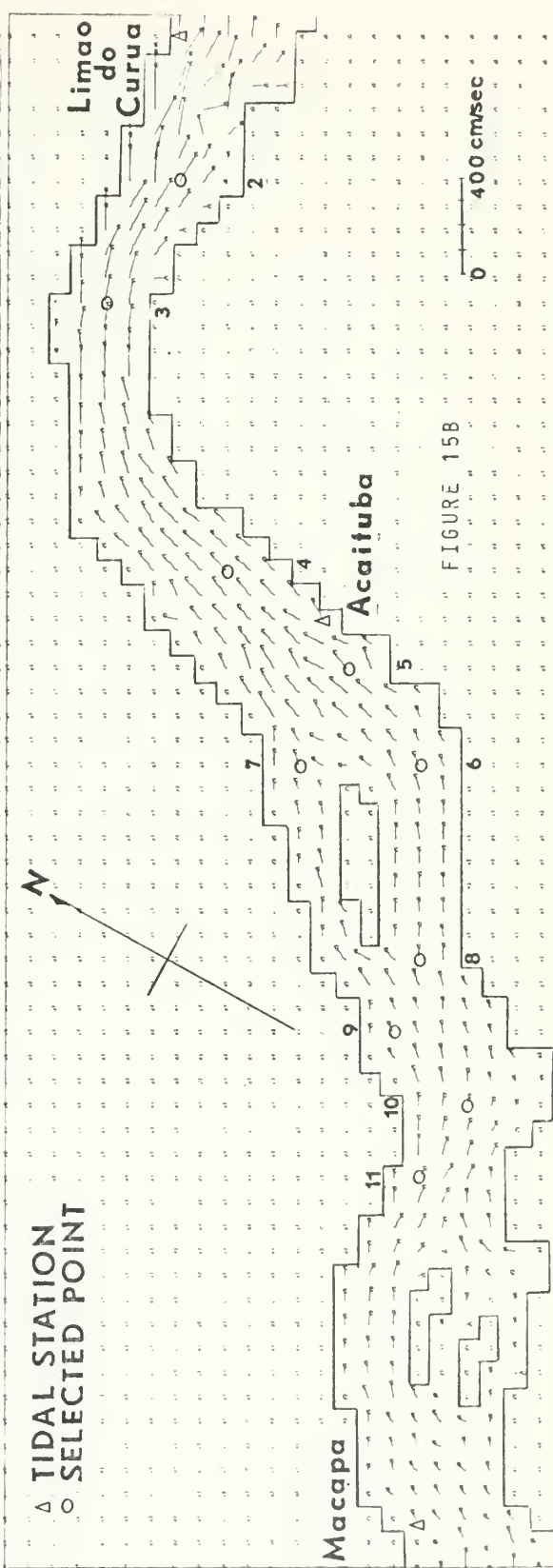
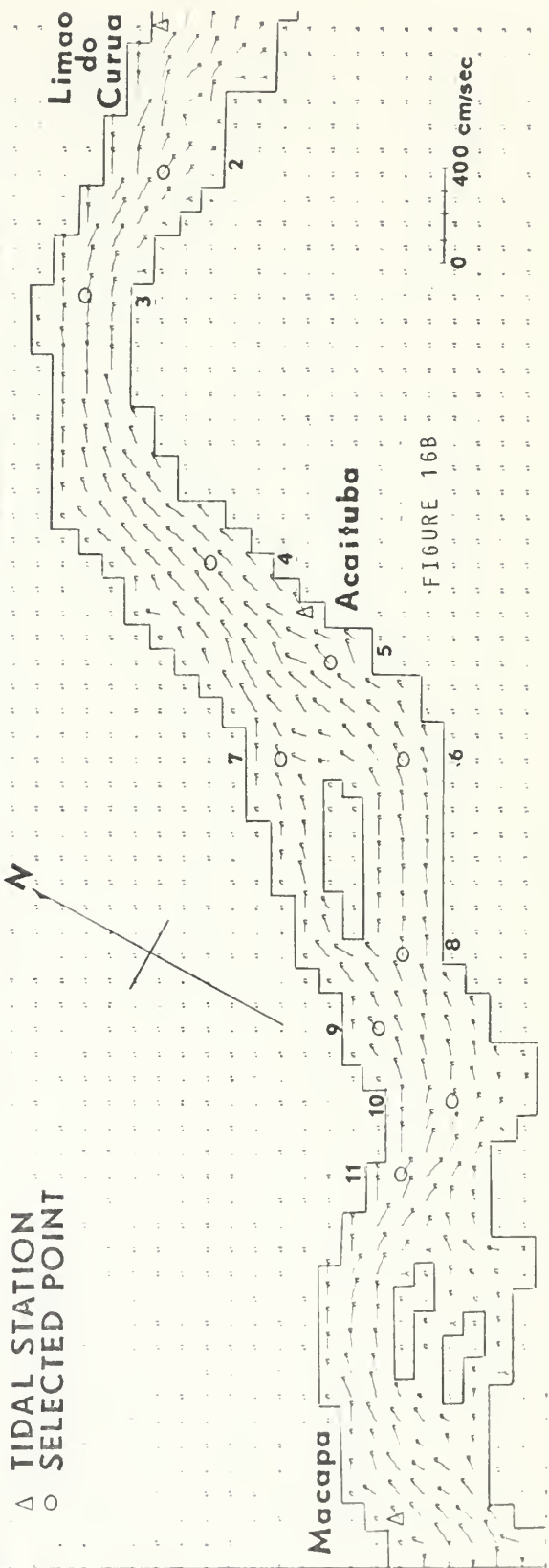
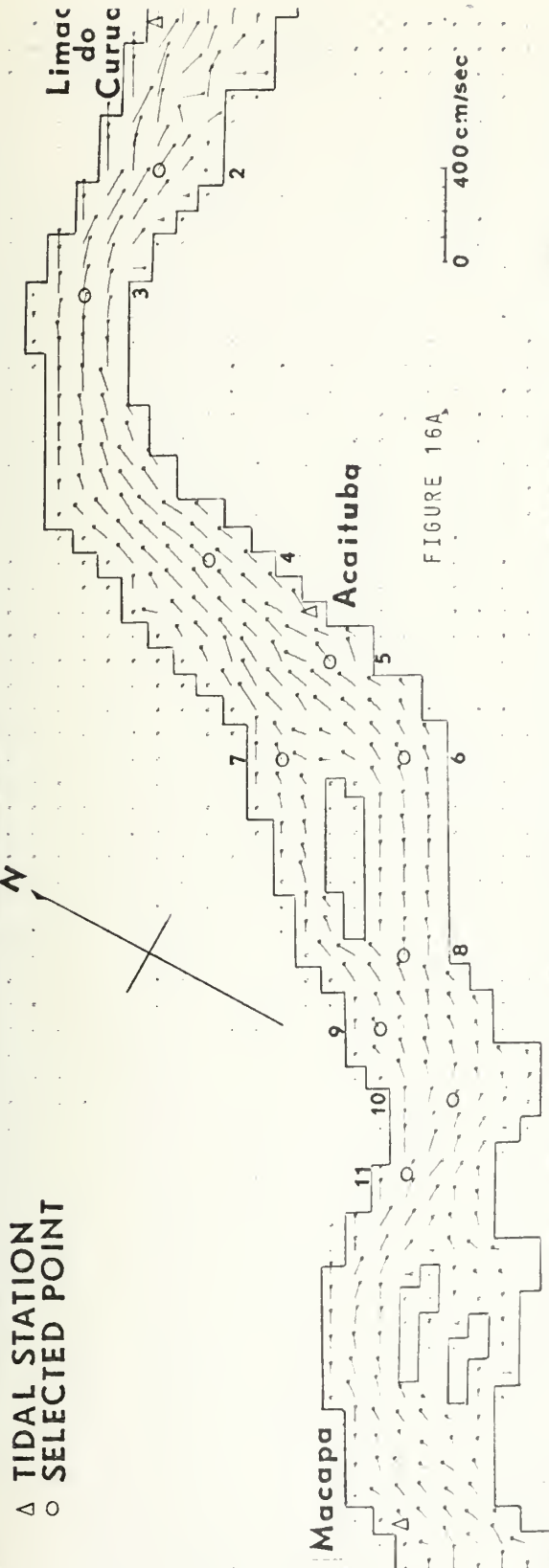


FIGURE 15B



Δ TIDAL STATION
○ SELECTED POINT

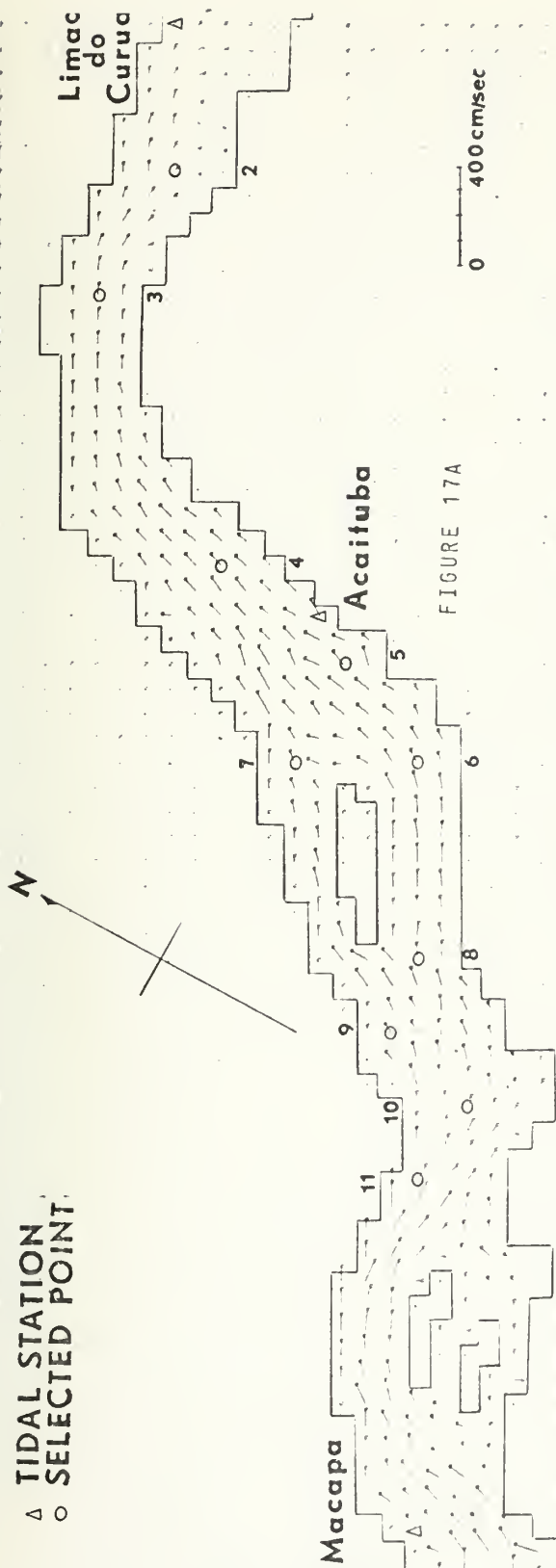


FIGURE 17A

Δ TIDAL STATION
○ SELECTED POINT

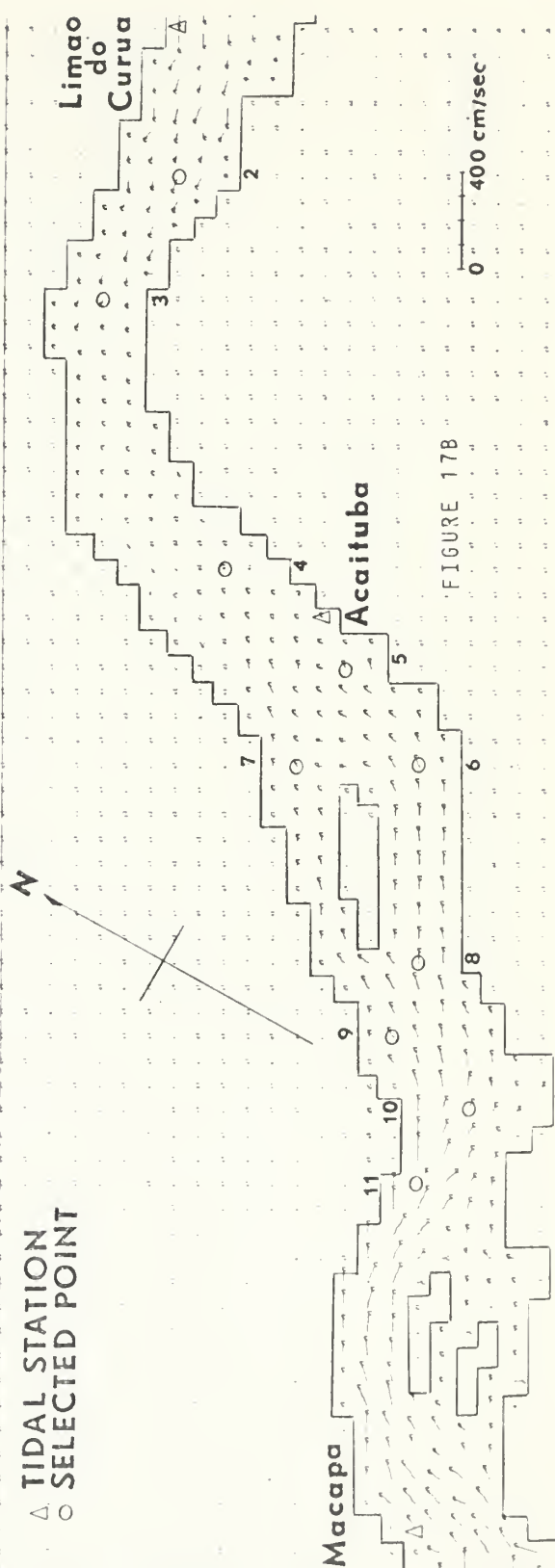
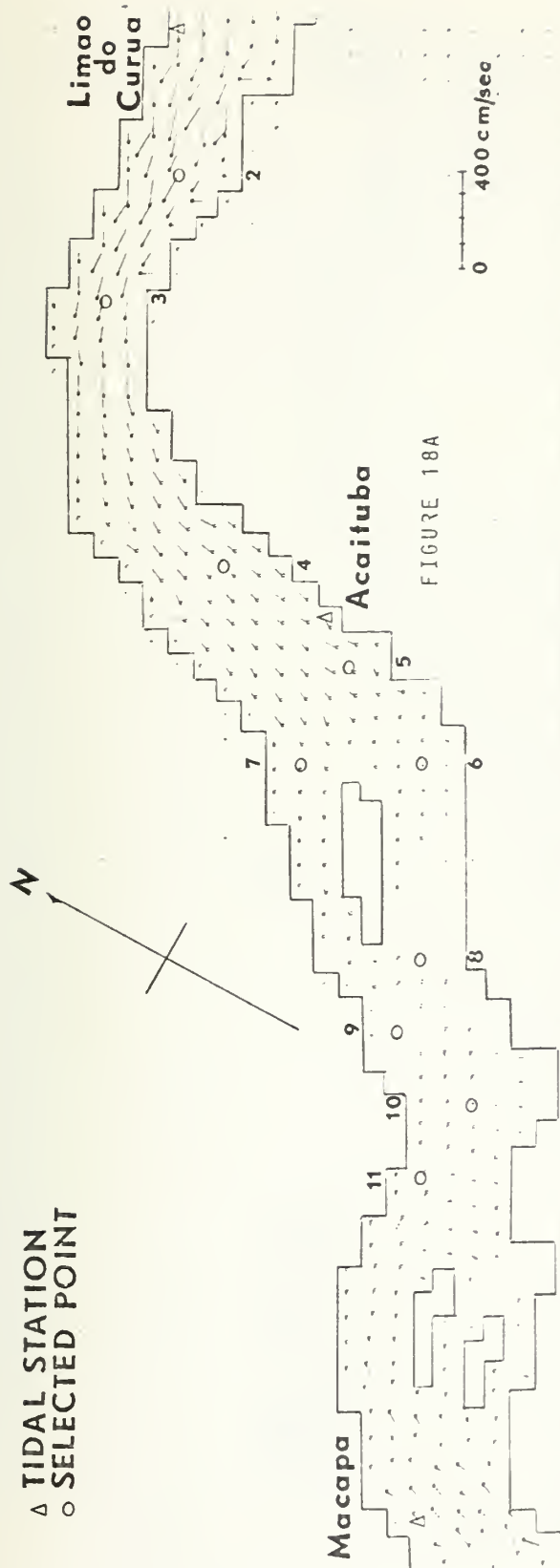
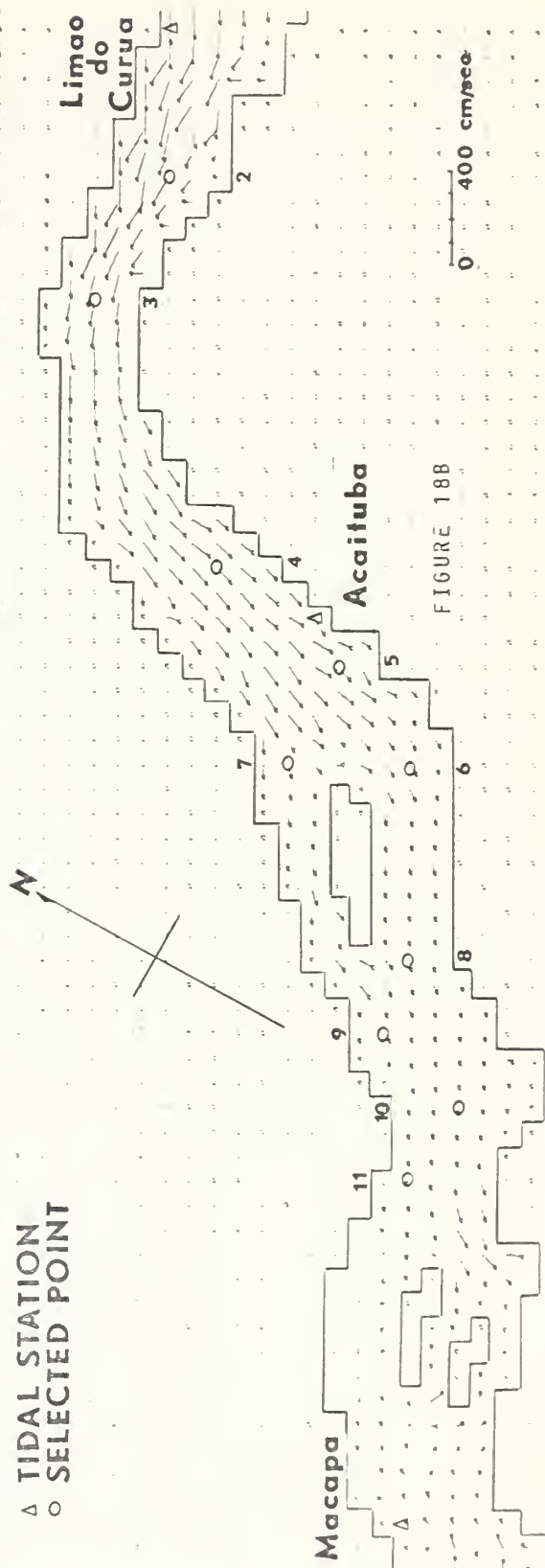


FIGURE 17B

Δ TIDAL STATION
○ SELECTED POINT



Δ TIDAL STATION
○ SELECTED POINT



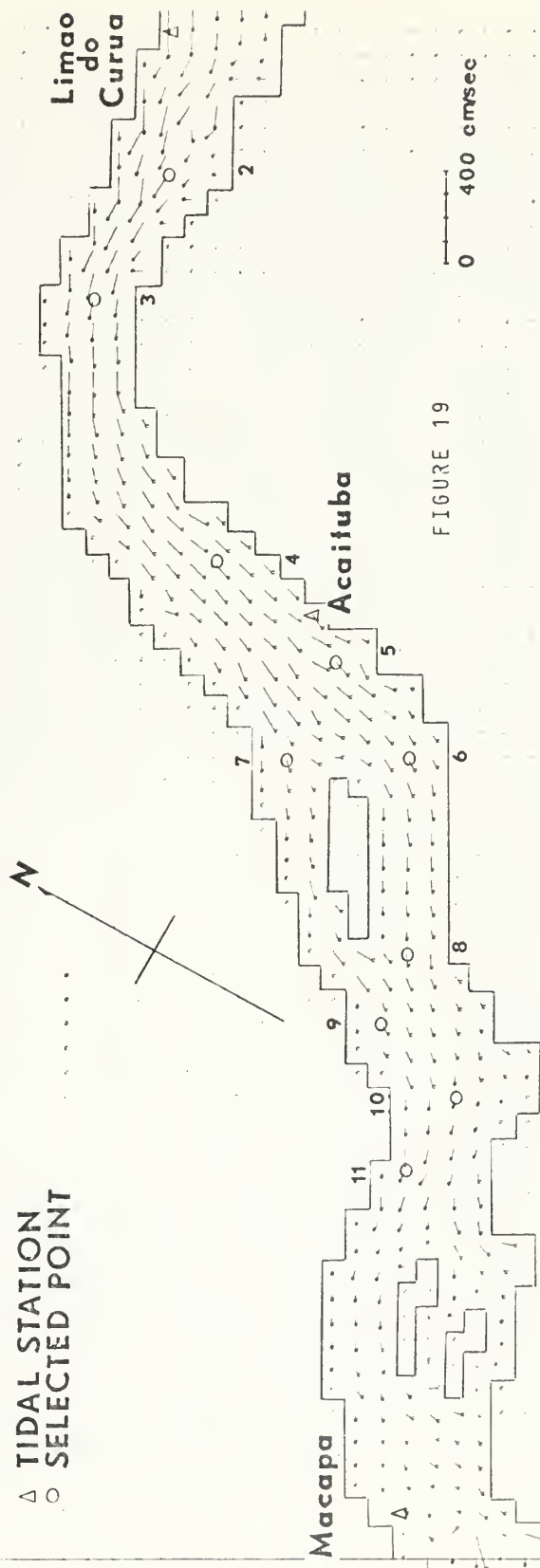


FIGURE 19

[illegible]

TABLE III. Computer Output for Water Elevation and Resultant Current Velocity and Direction in 12 Selected Locations

LIMAO DO CURVA

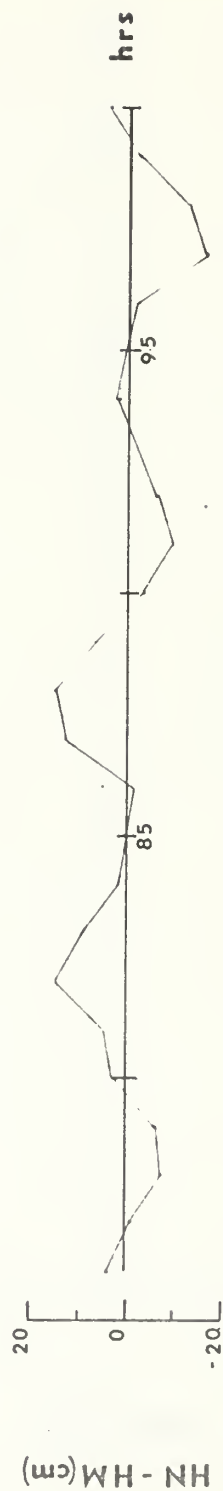
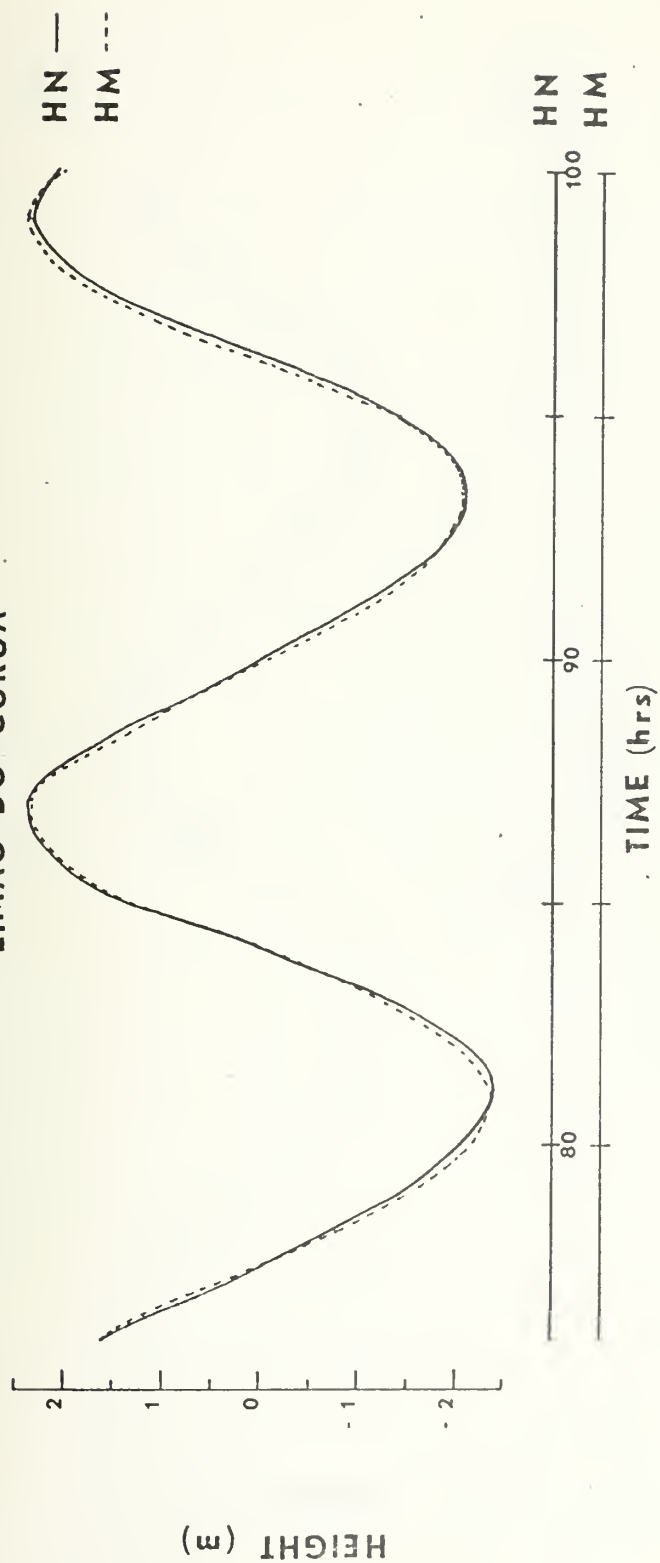


FIGURE 20

ACAITUBA

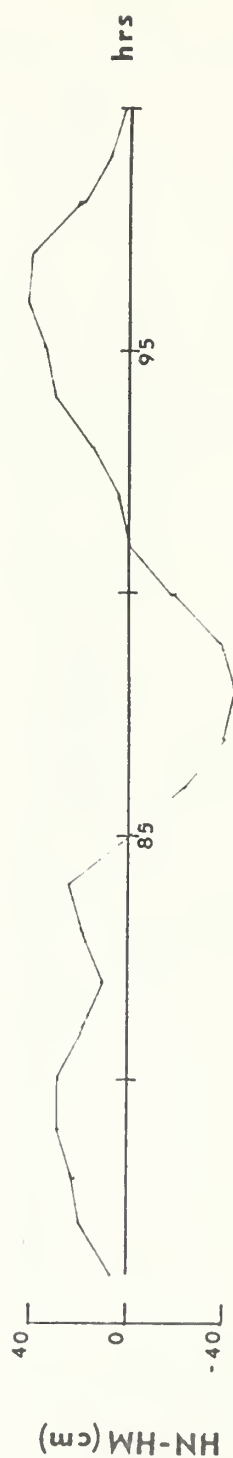
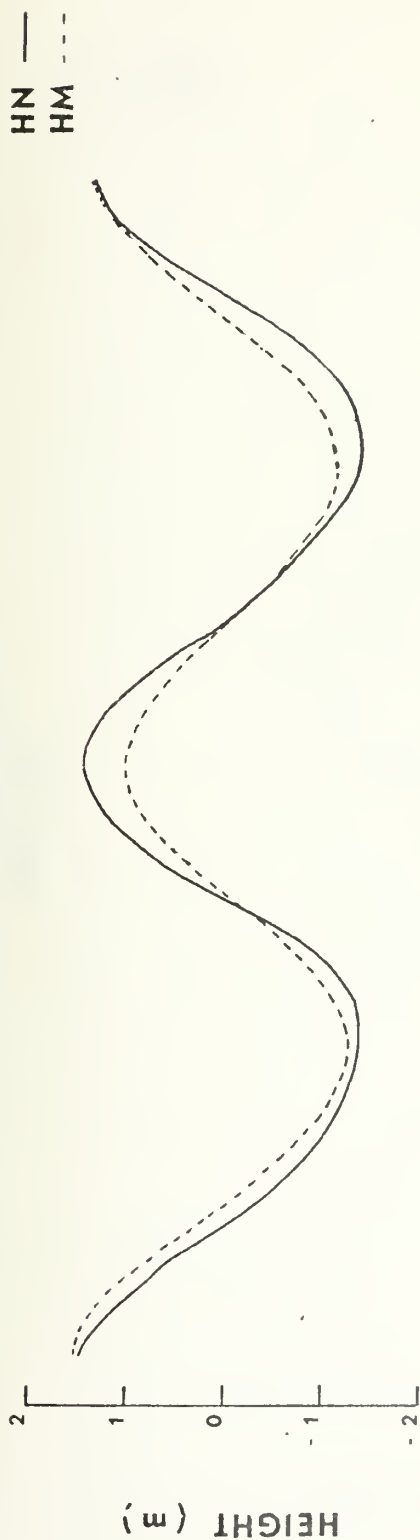


FIGURE 21

MACAPA

HN —
HM - -
HN1 - . -

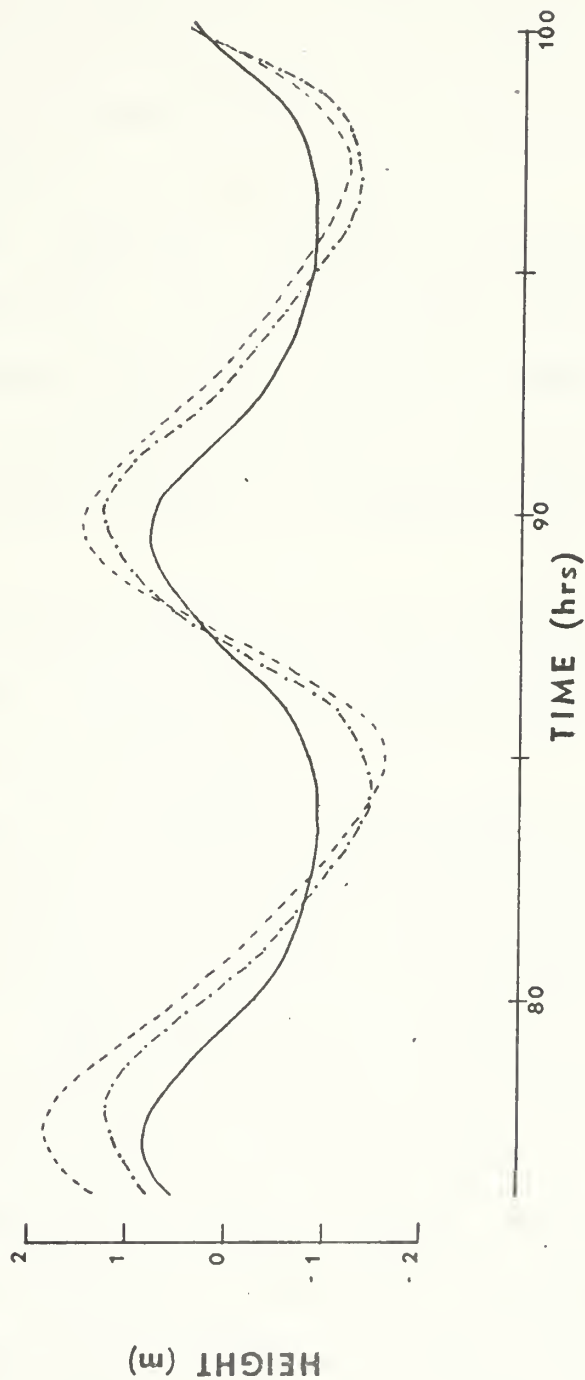


FIGURE 22

IV. DISCUSSION

Before discussing the results obtained upon applying the hydrodynamical-numerical prediction model developed by Hansen to the Amazon's North Channel, it is worthwhile to recall some of its properties or characteristics.

The model represents topographic features in terms of grid points. To obtain a good bathymetric representation a small mesh is required, which may sometimes lead to an extremely large array. It is therefore necessary to compromise between spatial resolution and the amount of computer core memory and time available.

The time resolution is also dependent upon availability of computer time; in general, the smaller the time step the greater the computer time required.

The flow is described by finite difference methods of solution of the equations of motion, which include terms of different orders and degrees, each one describing specific characteristics of the flow. These depend on the external forces applied, location, shape, bathymetry and properties inherent to the fluid. In describing the flow by these equations, it happens that some of the terms become dominant, so that others can be neglected or included in parameters such as K . In addition, Hansen's model neglects the advective non-linear terms, which appears not to cause problems if medium or coarse grids are used but seems to be significant for small grids, as mentioned before.

The finite difference method of solution of the equations of motion makes continuous computation impossible. The calculations are performed by time and spatial increments which can lead to enormous errors if the proper precautions are not taken. One example is that of the eddy diffusivity coefficient, which is affected directly by the grid size and the time step since it is defined in terms of spatial and temporal steps.

The action of viscosity in fluids is of a complicated nature. It may be assumed for the water motion in almost all tidal channels that a complete state of turbulence occurs, so that the flow is practically independent of the exact value of the Reynold's number. Because of the mathematical difficulties involved, the general equations of fluid motion, which include the viscous forces, are not generally solved in applied hydrodynamics. However, the result obtained by completely neglecting the bottom friction is, only under the most favorable circumstances, a satisfactory approximation to the actual fluid motion. Therefore, to determine the flow conditions in a channel, the influence of friction cannot be neglected [4].

To include friction, because the velocity varies in the horizontal as well as in the vertical directions in the cross-sections of the channel, there remains only the possibility of experimentally determining it by tuning the model so that predicted values match as closely as possible the observations.

In tidal channels and inland rivers, the river beds are usually irregular and form hydraulically rough surfaces, turbulence being generated by the irregularities of the bottom.

At the bottom the velocity is zero and increases in the vertical direction until it reaches a maximum value at some distance from the free surface. From this point to the surface the velocities decrease slightly. Observations in very wide channels have shown that the sides of the channel have practically no influence on the velocity distribution in the central region [4].

In engineering and practical problems the determination of the mean velocity in a cross-section is usually sufficient, thus making it necessary to have a relationship between the mean velocity and the frictional forces.

Hansen's model assumes that the bottom stress is directly dependent on U and V but only indirectly on X and t , and the same constant friction coefficient is used in all computations (for this case $r = 0.0029$).

Finally, the setting of the boundaries and the representation of the coast line and margins is also a matter of personal judgement, and because of this, often the representation of the real boundaries along the grid-points is somewhat difficult and may be questionable.

For our particular case, some facts have contributed to make adequate conclusions impossible. First, the river discharge is inputted as a permanent flow using an estimated value, because at the present time there are no available measurements of the discharge in the Amazon's North Channel. The distribution of the mean velocities in the cross-section was made at only five grid-points which received relatively large values, clearly affecting the resolution.

Second, there is insufficient adequate current measurements to provide a better adjustment of the predicted current velocities, either for the improvement of the estimated river discharge, neither for posterior verifications.

Third, the only tidal station in the middle portion of the Channel, ACAITUBA, had its constituents determined in a very short period of time, and the harmonic prediction for that station, using only few constituents, certainly is not the best. Furthermore, as mentioned before, this station is located about 2 km from the closest grid-point, which in turn is located in much deeper water.

In spite of these facts the model produced numerical results that, if not optimal, are at least acceptable.

The tides predicted at the northern station, LIMA DO CURUA, agreed with the harmonic prediction within 4% of the tidal range and no phase lag is observed. The maximum difference for the station at ACAITUBA is about 12% of the tidal range, and a phase lag of about 20 minutes is observed, but both may be attributed to the fact that the actual station is over shallower water than it is represented in the grid-point and to the distance from the grid-point to it.

At MACAPA, however, the results are unsatisfactory. This can be, at least partially, attributed to the fact that the grid size is too coarse to describe correctly the bottom topography and the cross-sections in the southern 18 km of the Channel, both very irregular. In fact, smoothing the large gradients between the depths at U- and V- grid-points of same

coordinate designation by making them shallower resulted in a better curve, as is illustrated in Fig. 22. No further improvement was tried because, due to the actual mesh size, the new "false-bottom" would not be realistic, and the procedure was abandoned. A similar situation is reported by Ramming [17] when modelling the Eider River in Germany: the first attempts to reproduce the tides in areas of very irregular cross-sections and depths were not satisfactory, in particular with regard to the steep flood part of the tidal curve. Differences of about 60 cm were recorded in a 3.8 m tidal range. Representing the cross-section by a fine structure of depth distribution, i.e., using a finer grid, led to results in which the maximum deviation was less than 10% of the tidal range and later improvements reduced this deviation to less than 1% of the tidal range [17].

The prediction of currents seems reasonable. At least at the four points where our current predictions were compared to actual observations made by the Brazilian Navy, in identical conditions of river stage, the results are quite satisfactory.

V. SUMMARY

The hydrodynamical-numerical prediction model developed by W. Hansen was applied to the North Channel of the Amazon River for prediction of tides and currents.

The tides predicted by the model agreed, in the worse case, to within 12% of the tidal variations at two stations, but the results at a third location weren't satisfactory. This is attributed to the fact that the irregular shape of the channel in the vicinity of this station was not adequately represented by the grid. Improvement in the results was obtained by smoothing the bottom at the U- and V- grid-points in order to decrease the gradients existing between these points, but no further adjustments were tried because they would be not realistic with the mesh size used. The currents predicted by the model appear to be satisfactorily reproduced, but more measurements are required to allow further conclusions.

It is the intention of the author to continue the investigations in this field to achieve improved results, both by decreasing the mesh dimensions and by using new measurements to be obtained in the near future. Continuation of the study will also be in the form of a two-layer HN-model which the author is preparing for the Amazon Estuary, for which more data and information are available.

APPENDIX A NUMERICAL PROGRAMS

HANSEN'S HYDRODYNAMICAL NUMERICAL PREDICTION MODEL APPLIED TO
THE NORTH CHANNEL OF THE AMAZON RIVER
LTC DR LUIZ ANTONIO DE CARVALHO FERRAZ - BRAZILIAN NAVY
NOTE: PLOTTING SUBROUTINES NOT INCLUDED IN THIS PROGRAM
PROGRAM 'NORTH-CHANNEL - AMAZON RIVER', MOUTH TO MACAPA
LIST OF PARAMETERS USED AND THEIR SIGNIFICANCE
A(I) = WIND FIELD CHARACTERISTICS
AH(I,J) = AMPLITUDE OF TIDAL CONST. AT INDIVIDUAL INPUT
POINTS
AL(I) = SPEED OF TIDAL CONSTITUENTS
AINC(I) = INTERMEDIATE PARAMETER IN INTERP. OF TIDES
ALPHA = SMOOTHING PARAMETER
ANG(N,M) = CURRENT DIRECTION
ARG(I,J) = ARGUMENT OF TIDAL CONSTITUENT
AUS = AUSTAU SCH COEFFICIENT
AI TO A5 = INTERMEDIATE PARAMETERS
B(I) = AMPLITUDES OF SECOND SET OF TIDAL CONSTITUENTS
BETA = 1 - ALPHA
BI TO B5 = INTERMEDIATE PARAMETERS
C = DRAG COEFFICIENT
CAINC = INTERMEDIATE PARAMETER IN INTERPOLATION OF TIDE
CAINC(U) = INTERMEDIATE PARAMETER IN INTERPOLATION OF TIDE
CAPAC(I,J) = G OR K OF FIRST SET OF TIDAL CONST.
CAPAP(I,J) = G OR K OF TIDAL CONST. AT INDIVI. INPUT POINT
CAPAB(I) = G OR K OF SECOND SET OF TIDAL CONST.
CNCU = INTERMEDIATE PARAMETER IN INTERPOLATION OF TIDE
CW = A COUNTER
C1 = WIND INDICATOR
C3 = INTERMEDIATE PARAMETER
DL = INTERMEDIATE SIZE
DT = HALF TIME STEP
H(I) = AMPLITUDES OF FIRST SET OF TIDAL CONSTITUENTS
HGV(N,M) = ACTUAL DEPTHS AT U POINTS
HTU(N,M) = ACTUAL DEPTHS AT V POINTS
HTV(N,M) = WATER DEPTHS AT U POINTS
HTZ(N,M) = WATER DEPTHS AT V POINTS
I,J,K,L = SYMBOLIC WATER-LAND DEPTHS AT Z POINTS
IU = A COUNTER
IUE = NUMBER OF WIND FIELDS
JA = TWICE NUMBER OF WIND FIELDS
JA=0 = INITIATION INDICATOR
JA=1 = COMPUTATIONS INITIALIZED AT ZERO FIELDS
KI = COMPUTATIONS INITIALIZED FROM PREVIOUS VALUES
KKE = TIDE INPUT INDICATOR
KO = NUMBER OF WIND FIELD CHARACTERISTICS
LA = NUMBER OF POINTS AT FIRST OPEN BOUNDARY
LE,LI,LU = NUMBER OF POINTS AT SECOND OPEN BOUNDARY
INDICATORS FOR REST CURRENT, DIFFUSION-TRANSPORT


```

LE=0 NO REST COMPUTATION
LE=1 REST COMPUTATION
LI=0 NO DIFFUSION COMPUTATION
LI=1 DIFFUSION COMPUTATION
LU=0 PERMANENT CURRENT NOT INPUTED
LU=1 PERMANENT CURRENT INPUT
LUP=0 INDICATOR FOR SPECIAL PLOTTING PROGRAM
LUP=1 NO PLOTTING
LUN=0 PLOTTING REQUIRING ADDITIONAL TAPE
LUN=1 INDICATOR FOR SIMPLIFIED DEPTH INPUT
LUN=0 DEPTHS AT U AND V POINTS DIFFERENT
LUN=1 DEPTHS AT U AND V POINTS EQUAL
M,N GRID INDEXES
ME,NE DELIMITERS OF GRID SIZE
MEH,NEH M-1,NE-1
MG,MK,ML M COORDINATES OF INPUT POINTS AT SEC,FIRST BDY
      AND INPUT OF PERMANENT CURRENTS
      WIND FIELD DELIMITERS
      COUNTER
MU,NU M,N COORDINATES OF SPECIAL POINTS OUTPUT
MUM,NON INDEXES
MZ,NZ M,N COORDINATES OF INPUT POINTS AT SEC,FIRST BDY
M1,M2 AND INPUT OF PERMANENT CURRENTS
NG,NK,NL AND INPUT OF SPECIAL OUTPUT POINTS
NURU INDEXES
N1,N2 U COMPONENT OF PERMANENT CURRENT
PERU(I) U COMPONENT OF PERMANENT CURRENT
PERV(I) V COMPONENT OF PERMANENT CURRENT
PREC(I) INTERMEDIATE FOR INTERPOL. OF TIDAL INPUT
RAD(N,M) FRICTION COEFFICIENT
RBETA CURRENT SPEED (RESULTANT)
ROL GEOSTROPHIC WIND COEFFICIENT
ROOT AIR DENSITY
SI,TW INTERMEDIATE
TIME WHEN WIND STOPS,STARTS
TIME COUNTER
TIC,T2 LENGTH OF COMPUTATION
TIL COUNT OF GRID WITH RESPECT TO TRUE NORTH
TIL TILT INTERVAL BETWEEN PRINTOUTS
UP(N,M) U COMPONENT OF CURRENT
V(N,M) V COMPONENT OF CURRENT
VPB(N,M) INTERMEDIATE FOR SMOOTHING AND AVERAGING
VRI,VUP INTERMEDIATE FOR SMOOTHING AND AVERAGING
VALE,VALQ,VAR1,VAUP INTERMEDIATE FOR AVERAGING
VLE,VLL,VLG,VLR,VUL INTERMEDIATES FOR AVERAGING
V1 NAMES OF SPECIAL OUTPUT POINTS
V2 TO V4 INTERMEDIATES FOR OUTPUT AT SPECIAL POINTS

```


1011	IF(T-TE) 7,240,240	AMZ 450
240	IF(LOP)1016,1016,241	AMZ 460
241	IF(LOP-5)1013,1016,1016	AMZ 470
7	T2=T2+T1	AMZ 480
8	CALL JOB2	AMZ 490
9	T=T+AI	AMZ 500
10	IF(T-TE)11,1012,1012	AMZ 510
11	IF(ABS (T-T2)-AI/2.)6,6,12	AMZ 520
12	GO TO 8	AMZ 530
1012	IF(LOP)13,13,1013	AMZ 540
1013	LOP=5	AMZ 550
1014	CALL JOB3	AMZ 560
1015	IF(LOP)1016,1016,1015	AMZ 570
1016	CONTINUE 2	AMZ 580
1017	END FILE 2	AMZ 590
14	REWIND 2	AMZ 600
15	CALL JOB5	AMZ 610
1017	IF(LOP)16,16,245	AMZ 620
245	CONTINUE	AMZ 630
1018	CONTINUE	AMZ 640
1016	STOP	AMZ 650
	END	AMZ 660
	SUBROUTINE JOB1	AMZ 670
	COMMON HTZ,HTU,HTV,Z,U,V,US,VS,RAD,ANG,XK,YK,NU,MU,NK,MK,AH,CAH,AP,	AMZ 680
	1PREC,ARG,PERU,PB,NC,ML,NZ,MZ,V1,UPB,VPB,S,A,V2,V3,V4,HGU,HGV,H,	AMZ 690
	2B,AL,CAPA,CAPB,A,INC,CAINC,TIT,IT,AUS,TAR,OTC,T1,T2,T4,TE,TW,AI,	AMZ 700
	3A2,A3,A4,DT,BETA,ALPHA,F,R,DL,G,C,C3,NE,ME,NEH,MEH,JA,IUE,KKE,NURU	AMZ 710
	4,SI,I,RBETA,CI,SIGMA,ROL,A5,RU,RV,KO,LI,LE,LU,KI,LOP,TRB,TRE,TIC,	AMZ 720
	5LUN,LA,TIL,LIV,LEET,POSN,POSN,DRI,STV,ETV,TINCV,STH,ETC,TINCH,CNCU	AMZ 730
	6,CAINC	AMZ 740
	DIMENSION HTZ(24,65),HTU(24,65),HTV(24,65),Z(24,65),U(24,65),V(24,	AMZ 750
	165),US(24,65),VS(24,65),RAD(24,65),ANG(24,65),XK(24,65),YK(24,65),	AMZ 760
	2NU(6),MU(6),NK(10),MK(10),AH(7,10),CAH(7,10),AP(7,10),ARG(7,10,	AMZ 770
	3),PERU(5),PERV(5),NL(5),NL(5),NZ(20),MZ(20),V1(20),UPB(24,65),	AMZ 780
	4)VPB(24,65),S(24,65),A(3),V2(20),V3(20),V4(20),HGU(24,65),HGV(24,65	AMZ 790
	5),H(7),B(7),AL(7),CAPA(7),CAPB(7),AINC(7),CAINC(7),NG(5),MG(5),	AMZ 800
	6,TIT(4),AUS(4),TAR(4),OTC(4)	AMZ 810
	DIMENSION MAP(24,65),TITLE(8),UPLOT(24,65),VPLOT(24,65)	AMZ 820
	READING OF VALUES AND INITIATION	AMZ 830
38	FORMAT(24F3.0)	AMZ 840
38	FORMAT(12F6.0)	AMZ 850
29	CONTINUE	AMZ 860
30	FORMAT(24I3)	AMZ 870
31	FORMAT(9F8.3)	AMZ 880
32	FORMAT(9F8.0)	AMZ 890
33	FORMAT(6E12.4)	AMZ 900
34	FORMAT(15(1X,A4))	AMZ 910
35	FORMAT(9F8.2)	AMZ 920


```

36 FFORMAT(14F5.1)
37 FFORMAT(7F10.7)
55 FFORMAT(F10.2)
READING OF INPUT DATA
1,LA,LUN,LIV,LEET,ME,KO,IUE,KKE,NURU,KI,LE,LU,LI,LOP
1006 READ 31,G,ALPHA,RBETA,C1,TIL
1008 READ 32,DF,TE,TW,T1,T2,SI,T,TRB,TRE
IF(LEET) 43,43,1008
1008 IF(LEET) 43,43,1008
43 READ 32,T4
READ 33,DL,F,SIGMA,R,ROL,C
READ 55,AUS(I)
READ 30,(NK(I),MK(I),I=1,N,KO)
READ 30,(NZ(I),WZ(I),I=1,NURU)
READ 30,(NU(I),MU(I),I=1,IUE)
READ 34,{V1(I),I=1,NURU)
NLN=1
1030 CW=1.
1036 CW=CW+I.
1032 NON=KKE+NON-1
1033 KKE=KKE+NON-1
1034 IF(C1-CW) 49,48,48
48 READ 35,(A(I),I=1,NON,KKE)
49 READ 36,(H(I),I=1,7)
50 READ 37,(AL(I),I=1,7)
51 READ 38,(CAPA(I),I=1,7)
52 READ 38,(HTZ(N,M),N=1,NE),M=1,ME)
DO 9956 N=13,17
HTZ(N,2)=-2.
9966 HTZ(N,1)=0.
1022 IF(LUN) 53,53,54
53 READ 38,((HTU(N,M),N=1,NE),M=1,ME)
54 READ 38,((HTV(N,M),N=1,NE),M=1,ME)
72 READ 30,(NU(I),NL(I),I=1,LU)
73 READ 36,(PERU(I),I=1,LU)
74 READ 36,(PERV(I),I=1,LU)
1005 CONTINUE
SETTING OF SOME COMPUTATIONAL PARAMETERS
60 BETA=(1.-ALPHA)/4.
61 A1=2.*DT A1
63 A3=R*A1
64 A4=DT/DL
65 A5=G*A4
66 C3=C*A1#10000.
67 NEH=NE-1
68 MEH=ME-1

```



```

1052 KKE = (IUE/2) * 3
INITIALIZATION OF THE ARRAYS WITH ZERO OR A SMALL VALUE
75 DO 100 N=1,NE
76 DO 100 M=1,ME
77 IF (HTZ(N,M)) 78,78,80
78 Z(N,M)=0.
79 VPB(N,M)=0.
79 GO TO 81
80 Z(N,M)=0.2
81 VPB(N,M)=0.2
81 IF (HTU(N,M)) 82,82,84
82 U(N,M)=0.
82 UPB(N,M)=0.
83 GO TO 85
84 U(N,M)=0.2
84 UPB(N,M)=0.2
84 IF (HTU(N,M)) 2085,2085,85
2085 IF (4000.-HTU(N,M)) = 4000.
85 HTU(N,M) = 4000.
86 V(N,M)=0.
86 VPB(N,M)=0.
87 GO TO 95
88 V(N,M)=0.2
88 VPB(N,M)=0.2
95 XK(N,M)=0.
96 YK(N,M)=0.
96 S(N,M)=0.
96 US(N,M)=0.
96 VS(N,M)=0.
96 IF (HTV(N,M).LE.0) GO TO 100
96 IF (4000.-HTV(N,M)) 2096,2096,100
2096 HTV(N,M) = 4000.
100 CONTINUE
DO 4100 N=1,NE
DO 4100 M=1,ME
IF (HTU(N,M).LT.100..AND.HTU(N,M).GT.0) HTU(N,M)=100.
IF (HTV(N,M).LT.100..AND.HTV(N,M).GT.0) HTV(N,M)=100.
4100 CONTINUE
DO 1200 J=1,KO
DO 1200 I=1,7
121 AH(I,J)=H(I)
122 CAPAP(I,J)=CAPA(I)
123 CONTINUE
124 CONTINUE
125 CONTINUE
PRINTING THE INPUT DATA FOR CHECKING PURPOSES
1131 PRINT 181,DT,DL
1132 PRINT 182,F,AUS(1)

```

AMZ1410
 AMZ1420
 AMZ1430
 AMZ1440
 AMZ1450
 AMZ1460
 AMZ1470
 AMZ1480
 AMZ1490
 AMZ1500
 AMZ1510
 AMZ1520
 AMZ1530
 AMZ1540
 AMZ1550
 AMZ1560
 AMZ1570
 AMZ1580
 AMZ1590
 AMZ1600
 AMZ1610
 AMZ1620
 AMZ1630
 AMZ1640
 AMZ1650
 AMZ1660
 AMZ1670
 AMZ1680
 AMZ1690
 AMZ1700
 AMZ1710
 AMZ1720
 AMZ1730
 AMZ1740
 AMZ1750
 AMZ1760
 AMZ1770
 AMZ1780
 AMZ1790
 AMZ1800
 AMZ1810
 AMZ1820
 AMZ1830
 AMZ1840
 AMZ1850
 AMZ1860
 AMZ1870
 AMZ1880


```

1133 PRINT 6168,R
1134 PRINT 183,ALPHA,C1
1135 PRINT 184,TE,T1,TW,SI
1136 PRINT 1142,TIL
1137 PRINT 1143,KI,LE,LU,LI,LOP,LUN,LA,LIV
1138 CCNTINUE
1139 PRINT 185,(NK(I),MK(I),I=1,KO)
1140 PRINT 186,H(1),H(2),H(3),H(4),H(5),H(6),H(7)
1141 PRINT 187,AL(1),AL(2),AL(3),AL(4),AL(5),AL(6),AL(7)
1142 PRINT 188,CAPA(1),CAPA(2),CAPA(3),CAPA(4),CAPA(5),CAPA(6),CAPA(7)
1143 MUM = IFIX (C1*3.)
1144 PRINT 189,(A(I),I=1,MUM)
1145 CCNTINUE
1146 IF(LU,1128,1128)
1147 PRINT 1145,(AL(I),ML(I),I=1,LU)
1148 PRINT 1147,(PERU(I),PERV(I),I=1,LU)
1149 CCNTINUE
1150 FFORMAT(5X,19HHALF TIME STEP DT =,F5.0,5H SEC,29X,20HHALF GRID SIZ
1151 LE DL =,E11.4,4H CM//)
1152 FFORMAT(5X,21HCORIOIS PARAMETER =,E12.4,5X,16HAUSTAUSCH COEF.=,
1153 FFORMAT(5X,27HSMOOTHING PARAMETER ALPHA =,F0.3,20X,19HWIND INDICATG
1154 IR CI =,F8.3//)
1155 FFORMAT(5X,15HCOMP. LENGTH ,F8.0,5X,15HOUTPUT INTERV.,F8.0,5X,15HW
1156 IN STARTS AT ,F8.0,5X,11HWIND STOPS ,F8.0,6HSECONDS,/)
1157 FFORMAT(5X,49H(N,M) COORDINATES OF INPUT POINTS AT THE BOUNDARY ,//
1158 15X,5(1H(,12.1H,12.1H,12.1H,12.1H,2X)//)
1159 FFORMAT(5X,AMPLITUDES OF TIDE CONST.,5X,7F10.1//)
1160 FFORMAT(5X,20HSPEDS OF TIDE CONST.,5X,7F10.7,/)
1161 FFORMAT(5X,21FKAPPAS OF TIDE CONST.,5X,7F10.7,/)
1162 FFORMAT(5X,25HIND,INTERV.,SPEED,DIR.,9F8.2,//5X,12F8.2,/)
1163 FFORMAT(5X,12HTILT OF GRID,5X,F4.0,/)
1164 13HLE=,I3,3HLE=,I3,3HLU=,I3,4HLOP=,I3,4HLUN=,I3,
1165 FFORMAT(//,8X,7I8)
1166 FFORMAT(18,7F8.0)
1167 FFORMAT(5X,24HCOORD.OF PERM.CURR.INPUT,//5X,5(1H(,I2,1H,12,1H),2X)
1168 1//)
1169 FFORMAT(5X,26HU AND V COMP.OF PERM.CURR.,/5X,5(1H(,F5.1,1H,F5.1,1H
1170 1),2X)/5X,5(1H(,F5.1,1H,2X)/5X,5(1H(,F5.1,1H,F5.1,1H),2X
1171 2)//)
1172 PRINT 6160,(N,N=1,15)
1173 PRINT 6161,(N,(H12(N,M),M=1,15),N=1,NE)
1174 PRINT 6162,(N,N=16,30)
1175 PRINT 6161,(N,(H12(N,M),M=16,30),N=1,NE)
1176 PRINT 6162,(N,N=31,45)
1177 PRINT 6161,(N,(H12(N,M),M=31,45),N=1,NE)
1178 PRINT 6162,(N,N=46,60)

```



```

DIMENSION HTZ(24,65),HTU(24,65),HTV(24,65),Z(24,65),U(24,65),V(24,
165),US(24,65),VS(24,65),RAD(24,65),ANG(24,65),XK(24,65),YK(24,65),
2NU(6),MU(6),NK(10),MK(10),AH(7,10),CAPAP(7,10),PREC(7,10),ARG(7,10
3),PERU(5),PERV(5),NL(5),ML(5),NZ(20),MZ(20),V1(20),VPB(24,65),
4VPB(24,65),S(24,65),A(3),V2(20),V3(20),V4(20),HGU(24,65),HGV(24,65
5),H(7),B(7),AL(7),CAPA(7),CAPB(7),AINC(7),CAINC(7),NG(5),MG(5),
6TIT(7),AUS(4),TAR(4),OTC(4)
DIMENSION MAP(24,65),TITLE(8),UPLOT(24,65),VPLOT(24,65)
COMPUTATIONS
TIDAL INPUT ARE THOSE OF 'LIMAO DO CURUA' AND SEVEN COMPONENTS ARE
THE TIDES THE INPUT WAS DONE AT THE SECOND COLUMN OF THE COMPUTATIONAL
USED, AT M EQUALS TWO
GRID, AT M EQUALS TWO
309 CONTINUE
310 DO 328 I=1,7
311 DO 328 J=1,KO
312 PREC(I,J)=AL(I)*T-CAPAP(I,J)
313 IF(PREC(I,J))314,321,315
314 IF(PREC(I,J))-6.283185)318,318,316
315 PREC(I,J)=6.283185+PREC(I,J)
316 PREC(I,J)=PREC(I,J)-6.283185
317 GO TO 315
318 IF(PREC(I,J))-1.570796)321,321,319
319 IF(PREC(I,J))-3.141593)323,323,320
320 IF(PREC(I,J))-4.712389)325,325,327
321 ARG(I,J)=COS (PREC(I,J))
322 GO TO 328
323 ARG(I,J)=-COS (3.141593-PREC(I,J))
324 GO TO 328
325 ARG(I,J)=-COS (PREC(I,J)-3.141593)
326 GO TO 328
327 ARG(I,J)=COS (6.283185-PREC(I,J))
328 CONTINUE
329 DO 384 I=1,KO
330 N=NK(I)
331 M=NK(I)
332 Z(N,M)=AH(1,I)*ARG(1,I)+AH(2,I)*ARG(2,I)+AH(3,I)*ARG(3,I)+AH(4,I)*
333 ARG(4,I)+AH(5,I)*ARG(5,I)+AH(6,I)*ARG(6,I)+AH(7,I)*ARG(7,I)
334 CONTINUE
335 CONTINUE
336 Z(N,M)=AH(1,I)*ARG(1,I)+AH(2,I)*ARG(2,I)+AH(3,I)*ARG(3,I)+AH(4,I)*
337 ARG(4,I)+AH(5,I)*ARG(5,I)+AH(6,I)*ARG(6,I)+AH(7,I)*ARG(7,I)
338 CONTINUE
339 DO 394 N=1,NE
340 DO 394 M=1,ME
341 VPB(N,M)=0.
342 VPB(N,M)=0.
343 CONTINUE
344 CONTINUE
345 DO 523 N=1,NE
346 DO 523 M=1,ME
347 IF(HTZ(N,M))523,523,503

```



```

503 IF(1-N) 504,507,504
504 IF(HTZ(N-1,M)) 505,507,505
505 VAUP=Z(N-1,M)
506 GO TO 508
507 VAUP=Z(N,M)
508 IF(NE-N) 509,512,509
509 IF(HTZ(N+1,M)) 510,512,510
510 VALO=Z(N+1,M)
511 GO TO 513
512 VALO=Z(N,M)
513 IF(1-M) 514,516,514
514 IF(HTZ(N,M-1)) 1514,516,1514
1514 VALE=Z(N,M-1)
515 GO TO 517
516 VALE=Z(N,M)
517 IF(ME-M) 518,521,518
518 IF(HTZ(N,M+1)) 519,521,519
519 VARI=Z(N,M+1)
520 GO TO 522
521 VARI=Z(N,M)
522 VPB(N,M)=ALPHA*Z(N,M)+BETA*(VAUP+VALO+VALE+VARI)
523 CONTINUE
530 DO 535 N=2,NEH
531 DO 535 M=3,ME
532 IF(HTZ(N,M)) 535,535,2533
2533 IF(HTZ(N,M))-3.1535,535,533
533 Z(N,M)=VPB(N,M)-A4*(HGU(N,M)*U(N,M)-1)+HGV(N-1,M)*V(N,M)
535 CONTINUE
COMPUTATION OF REAL DEPTHS
1537 DO 1543 N=1,NEH
1538 DO 1543 M=1,MEH
1539 IF(HTU(N,M)) 1541,1541,1540
1540 IF(HTU(N,M))=HTU(N,M)+(Z(N,M)+Z(N,M+1))/2.
1541 IF(HTV(N,M)) 1543,1542
1542 HGV(N,M)=HTV(N,M)+(Z(N,M)+Z(N+1,M))/2.
1543 CONTINUE
CHECKING OF DRYING OF TIDAL FLATS
1560 DO 1568 N=1,NE
1561 DO 1568 M=1,ME
1562 IF(HTU(N,M)) 1565,1565,1563
1563 IF(HGU(N,M)-10.) 1564,1564,1565
1564 HGU(N,M)=-3.
1565 IF(HTV(N,M)) 1568,1568,1566
1566 IF(HGV(N,M)-10.) 1567,1567,1568
1567 HGV(N,M)=-3.
1568 CONTINUE

```

```

AMZ33330
AMZ33340
AMZ33350
AMZ33360
AMZ33370
AMZ33380
AMZ33390
AMZ3400
AMZ3410
AMZ3420
AMZ3430
AMZ3440
AMZ3450
AMZ3460
AMZ3470
AMZ3480
AMZ3490
AMZ3500
AMZ3510
AMZ3520
AMZ3530
AMZ3540
AMZ3550
AMZ3560
AMZ3570
AMZ3580
AMZ3590
AMZ3600
AMZ3610
AMZ3620
AMZ3630
AMZ3640
AMZ3650
AMZ3660
AMZ3670
AMZ3680
AMZ3690
AMZ3700
AMZ3710
AMZ3720
AMZ3730
AMZ3740
AMZ3750
AMZ3760
AMZ3770
AMZ3780
AMZ3790
AMZ3800

```



```

COMPUTATION OF U-BAR
540 DO 585 N=2,NEH
541 DO 585 M=2,MEH
542 IF (HTU(N,M)) 585,585,543
543 IF (1-N) 544,547,544
544 IF (HTU(N-1,M)) 545,547,545
545 VUP=U(N-1,M)
546 GO TO 548
547 VUP=U(N,M)
548 IF (NE-N) 549,552,549
549 IF (HTU(N+1,M)) 550,552,550
550 VLO=U(N+1,M)
551 GO TO 553
552 VLO=U(N,M)
553 IF (1-M) 554,557,554
554 IF (HTU(N,M-1)) 555,557,555
555 VLE=U(N,M-1)
556 GO TO 558
557 VLE=U(N,M)
558 IF (ME-M) 559,562,559
559 IF (HTU(N,M+1)) 560,562,560
560 VRI=U(N,M+1)
561 GO TO 563
562 VRI=U(N,M)
563 UPB(N,M)=ALPHA*U(N,M)+BETA*(VUP+VLO+VLE+VRI)
COMPUTATION OF V-STAR
564 IF (HTV(N-1,M)) 565,569,565
565 VUL=V(N-1,M)
566 IF (HTV(N-1,M+1)) 567,570,567
567 VUR=V(N-1,M+1)
568 GO TO 571
569 VUL=V(N-1,M+1)
570 VUR=VUL
571 IF (HTV(N,M)) 572,576,572
572 VLL=V(N,M)
573 IF (HTV(N,M+1)) 574,577,574
574 VLR=V(N,M+1)
575 GO TO 578
576 VLL=V(N,M+1)
577 VLR=VLL
578 VPB(N,M)=(VUL+VLL+VUR+VLR)/4.
COMPUTATION OF U
585 CONTINUE
586 DO 595 N=2,NEH
587 DO 595 M=2,MEH
588 IF (HTU(N,M)) 595,595,1570
1570 IF (HGU(N,M)-3.) 595,1571,589
1571 VPB(N,M)=0.

```

AMZ3810
 AMZ3820
 AMZ3830
 AMZ3840
 AMZ3850
 AMZ3860
 AMZ3870
 AMZ3880
 AMZ3890
 AMZ3900
 AMZ3910
 AMZ3920
 AMZ3930
 AMZ3940
 AMZ3950
 AMZ3960
 AMZ3970
 AMZ3980
 AMZ3990
 AMZ4000
 AMZ4010
 AMZ4020
 AMZ4030
 AMZ4040
 AMZ4050
 AMZ4060
 AMZ4070
 AMZ4080
 AMZ4090
 AMZ4100
 AMZ4110
 AMZ4120
 AMZ4130
 AMZ4140
 AMZ4150
 AMZ4160
 AMZ4170
 AMZ4180
 AMZ4190
 AMZ4200
 AMZ4210
 AMZ4220
 AMZ4230
 AMZ4240
 AMZ4250
 AMZ4260
 AMZ4270
 AMZ4280


```

1572 GO TO 595
1589 IF (UPB(N,M)*UPB(N,M))595,590,591
1590 IF (VPB(N,M)*VPB(N,M))595,595,591
1591 ROOT=SQRT (UPB(N,M)*UPB(N,M)+VPB(N,M)*VPB(N,M))
1592 GRZ=A3*ROOT
1593 VPB(N,M)= (1. - GRZ/HGU(N,M))*UPB(N,M) + A2*VPB(N,M) - A5*
1 (Z(N,M+1) - Z(N,M)) + XK(N,M)
595 CONTINUE
SPECIAL INFLOW SETTING
U-COMPONENT OF SPECIAL INFLOW SETTING
THE RIVER INFLOW WAS INTRODUCED AT THE SECTION PERPENDICULAR TO
MACAPA
1590 IF (LU)900,900,1591
1591 DO 1595 I=1,LU
1592 N=NL(I)
1593 M=ML(I)
1594 VPB(N,M) = PERU(I) + VPB(N,M)
1595 CONTINUE
3596 DO 3600 N=1,NE
3597 IF (HTU(N,1))3600,3600,3597
3598 IF (HTU(N,2))3600,3600,3598
3600 VPB(N,1)=VPB(N,2)*HTU(N,1)/HTU(N,2)
COMPUTATION OF U-STAR
900 DO 918 N=1,NEH
901 DO 918 M=2,ME
902 IF (HIV(N,M))918,918,903
903 IF (HTU(N,M-1))904,908,904
904 VUL=U(N,M-1)
905 IF (HTU(N+1,M-1))906,909,906
906 VLL=U(N+1,M-1)
907 GO TO 910
908 VUL=U(N+1,M-1)
909 VLI=VUL
910 IF (HTU(N,M))911,915,911
911 VUR=U(N,M)
912 IF (HTU(N+1,M))913,916,913
913 VLR=U(N+1,M)
914 GO TO 917
915 VUR=U(N+1,M)
916 VLR=VUR
917 UPB(N,M)=(VUL+VLL+VUR+VLR)/4.
918 CONTINUE
TRANSFER OF NEW U INTO PROPER ARRAY
GO TO 920
920 DO 924 N=1,NE
921 DO 924 M=1,ME
922 IF (HTU(N,M))924,924,923

```

AMZ4290
 AMZ4300
 AMZ4310
 AMZ4320
 AMZ4330
 AMZ4340
 AMZ4350
 AMZ4360
 AMZ4370
 AMZ4380
 AMZ4390
 AMZ4400
 AMZ4410
 AMZ4420
 AMZ4430
 AMZ4440
 AMZ4450
 AMZ4460
 AMZ4470
 AMZ4480
 AMZ4490
 AMZ4500
 AMZ4510
 AMZ4520
 AMZ4530
 AMZ4540
 AMZ4550
 AMZ4560
 AMZ4570
 AMZ4580
 AMZ4590
 AMZ4600
 AMZ4610
 AMZ4620
 AMZ4630
 AMZ4640
 AMZ4650
 AMZ4660
 AMZ4670
 AMZ4680
 AMZ4690
 AMZ4700
 AMZ4710
 AMZ4720
 AMZ4730
 AMZ4740
 AMZ4750
 AMZ4760


```

923 U(N,M) = VPB(N,M)
924 CONTINUE
COMPUTATION OF V-BAR
930 DO 954 N=1,NE
931 DO 954 M=1,ME
932 IF (HTV(N,M)) 954,954,933
933 IF (1-N) 934,937,934
934 IF (HTV(N-1,M)) 935,937,935
935 VUP=V(N-1,M)
936 GO TO 938
937 VUP=V(N,M)
938 IF (NE-N) 939,942,939
939 IF (HTV(N+1,M)) 940,942,940
940 VLO=V(N+1,M)
941 GO TO 943
942 VLO=V(N,M)
943 IF (1-M) 944,947,944
944 IF (HTV(N,M+1)) 945,947,945
945 VLE=V(N,M-1)
946 GO TO 948
947 VLE=V(N,M)
948 IF (ME-M) 949,952,949
949 IF (HTV(N,M+1)) 950,952,950
950 VRI=V(N,M+1)
951 GO TO 953
952 VRI=V(N,M)
953 VPB(N,M)=ALPHA*V(N,M)+BETA*(VUP+VLO+VLE+VRI)
954 CONTINUE
COMPUTATION OF V
960 DO 969 N = 2,NEH
961 DO 969 M=1,MEH
962 IF (HTV(N,M)) 969,969,1990
1990 IF (HGV(N,M)-3.) 969,1991,963
1991 V(N,M)=0.
1992 GO TO 969
963 IF (VPB(N,M))*VPB(N,M)) 969,964,965
964 IF (UPB(N,M))*UPB(N,M)) 969,969,965
965 ROOT=SQRT((VPB(N,M))*VPB(N,M)+UPB(N,M))*UPB(N,M))
966 GRZ=A3*ROOT
967 V(N,M) = (1. - GRZ/HGV(N,M))*VPB(N,M) - A2*UPB(N,M) - A5*(Z(N,M)
1 - Z(N+1,M)) + YK(N,M)
969 CONTINUE
V-COMPOnent OF SPECIAL INFLOW SETTING
DC 6000 I=1,4
N=NL(I)
M=ML(I)
V(N,M) = PERV(I) + V(N,M)
6000 CONTINUE

```

AMZ4770
 AMZ4780
 AMZ4790
 AMZ4800
 AMZ4810
 AMZ4820
 AMZ4830
 AMZ4840
 AMZ4850
 AMZ4860
 AMZ4870
 AMZ4880
 AMZ4890
 AMZ4900
 AMZ4910
 AMZ4920
 AMZ4930
 AMZ4940
 AMZ4950
 AMZ4960
 AMZ4970
 AMZ4980
 AMZ4990
 AMZ5000
 AMZ5010
 AMZ5020
 AMZ5030
 AMZ5040
 AMZ5050
 AMZ5060
 AMZ5070
 AMZ5080
 AMZ5090
 AMZ5100
 AMZ5110
 AMZ5120
 AMZ5130
 AMZ5140
 AMZ5150
 AMZ5160
 AMZ5170
 AMZ5180
 AMZ5190
 AMZ5200
 AMZ5210
 AMZ5220
 AMZ5230
 AMZ5240


```

300 CONTINUE
472 CONTINUE
RETURN
END
SUBROUTINE JOB3
COMMON HTZ,HTU,HTV,Z,U,V,US,VS,RAD,ANG,XK,YK,NU,MU,NK,MK,AH,CAPAP,
1PRC,AKG,PERU,NL,ML,MZ,VI,UPB,VPB,S,A,V2,V3,V4,HGU,HGV,H,
2B,AL,CAPA,CAPB,AINC,CAINC,NG,MG,TIT,AUS,IAR,OTC,T1,I2,I4,TE,TW,A1,
3A2,A3,A4,D1,BETA,ALPHA,F,R,DL,G,C,C3,NE,ME,NEH,MEH,JA,IUE,KKE,NURU
4SI,T,IRBETA,CI,SIGMA,ROL,A5,RU,RV,KO,LI,LE,LU,KI,LOP,IRB,TRE,TIC,
5LUN,LA,TIL,LIV,LEET,POSN,POSMDRI,STV,ETV,TINCV,STH,ETC,TINCH,CNCU
6CAINC
DIMENSION HTZ(24,65),HTU(24,65),HTV(24,65),Z(24,65),U(24,65),V(24,
165),US(24,65),VS(24,65),RAD(24,65),ANG(24,65),XK(24,65),YK(24,65),
2NU(6),MU(6),NK(10),MK(10),AH(7,10),CAPAP(7,10),PREC(7,10),ARG(7,10
3),PERU(5),PERV(5),NL(5),ML(5),NZ(20),MZ(20),V1(20),UPB(24,65),
4VPB(24,65),S(24,65),A1(3),V2(20),V3(20),V4(20),HGU(24,65),HGV(24,65
5),H(7),B(7),AL(7),CAPA(7),CAPB(7),AINC(7),CAINC(7),NG(5),MG(5),
6TIT(4),AUS(4),TAR(4),OTC(4)
DIMENSION MAP(24,65),TITLE(8),UPLOT(24,65),VPLT(24,65)
WRITING OF OUTPUT FIELDS
1605 FORMAT(/,8X,5I8)
1604 FORMAT(18,5F8.0,/)
32 FORMAT(9F8.0)
601 CONTINUE
610 PRINT602,T,(M,N=1,15)
611 PRINT604,(N,(Z(N,M),M=1,15),N=1,NE)
612 PRINT605,(N,N=16,30)
613 PRINT604,(N,(Z(N,M),M=16,30),N=1,NE)
PRINT605,(N,N=31,45)
PRINT604,(N,(Z(N,M),M=31,45),N=1,NE)
PRINT605,(N,N=46,60)
PRINT604,(N,(Z(N,M),M=46,60),N=1,NE)
PRINT1605,(N,N=61,65)
PRINT1604,(N,(Z(N,M),M=61,65),N=1,NE)
PRINT1604,(N,(Z(N,M),M=61,65),N=1,NE)
COMPUTATION OF SPEED AND DIRECTION FROM U AND V COMPONENTS
614 DO 639 N=1,NE
617 DO 639 M=1,ME
618 IF(V(N,M))620,619,620
619 IF(U(N,M))620,622,620
620 RAD(N,M)=SQRT (ABS (V(N,M))**2+ABS (U(N,M))**2)
621 GO TO 625
622 RAD(N,M)=0.
623 ANG(N,M)=0.
624 GO TO 639
625 ANG(N,M)=ABS (ARSIN(V(N,M)/RAD(N,M)))
626 ANG(N,M)=ANG(N,M)/360./6.2831853073)
627 IF(V(N,M))629,628,628

```

AMZ5250
 AMZ5260
 AMZ5270
 AMZ5280
 AMZ5290
 AMZ5300
 AMZ5310
 AMZ5320
 AMZ5330
 AMZ5340
 AMZ5350
 AMZ5360
 AMZ5370
 AMZ5380
 AMZ5390
 AMZ5400
 AMZ5410
 AMZ5420
 AMZ5430
 AMZ5440
 AMZ5450
 AMZ5460
 AMZ5470
 AMZ5480
 AMZ5490
 AMZ5500
 AMZ5510
 AMZ5520
 AMZ5530
 AMZ5540
 AMZ5550
 AMZ5560
 AMZ5570
 AMZ5580
 AMZ5590
 AMZ5600
 AMZ5610
 AMZ5620
 AMZ5630
 AMZ5640
 AMZ5650
 AMZ5660
 AMZ5670
 AMZ5680
 AMZ5690
 AMZ5700
 AMZ5710
 AMZ5720

AMZ5730
AMZ5740
AMZ5750
AMZ5760
AMZ5770
AMZ5780
AMZ5790
AMZ5800
AMZ5810
AMZ5820
AMZ5830
AMZ5840
AMZ5850
AMZ5860
AMZ5870
AMZ5880
AMZ5890
AMZ5900
AMZ5910
AMZ5920
AMZ5930
AMZ5940
AMZ5950
AMZ5960
AMZ5970
AMZ5980
AMZ5990
AMZ6000
AMZ6010
AMZ6020
AMZ6030
AMZ6040
AMZ6050
AMZ6060
AMZ6070
AMZ6080
AMZ6090
AMZ6100
AMZ6110
AMZ6120
AMZ6130
AMZ6140
AMZ6150
AMZ6160
AMZ6170
AMZ6180
AMZ6190
AMZ6200

```

628 IF(U(N,M))631,636,636
629 IF(U(N,M))633,633,630
630 GO TO 635
631 ANG(N,M)=180.-ANG(N,M)
632 GO TO 636
633 ANG(N,M)=180.+ANG(N,M)
634 GO TO 636
635 ANG(N,M)=360.-ANG(N,M)
636 ANG(N,M)=(90.-ANG(N,M)) - TIL
637 IF(ANG(N,M))638,639,639
638 ANG(N,M)=360.+ANG(N,M)
639 GO TO 637
2638 CONTINUE
2639 IF(T.LT.230400.)GO TO 2000
PREPARATION OF CURRENT COMPONENTS TO BE PLOTTED IN GRID
DO 6000 N=1,NE
DO 6000 M=1,ME
UPLUT(N,M)=RAD(N,M)*SIN((ANG(N,M)+208.)*0.0174533)
VPLOT(N,M)=-RAD(N,M)*COS((ANG(N,M)+208.)*0.0174533)
6000 READ(5,500) TITLE
500 FORMAT (A4)
CALL STREAM(24,65,VPLOT,UPLOT,MAP,1.0,1.0,4,.51,TITLE,3.00,3.00,
12,1.400.)
2000 CONTINUE
PRINTING OF OUTPUT FIELDS
650 PRINT 607,(N,RAD(N,M),ANG(N,M),M=1,10),N=1,NE)
651 PRINT 606,(N,RAD(N,M),ANG(N,M),M=11,20),N=1,NE)
652 PRINT 609,(N,RAD(N,M),ANG(N,M),M=21,30),N=1,NE)
653 PRINT 608,(N,RAD(N,M),ANG(N,M),M=31,40),N=1,NE)
PRINT 608,(N,RAD(N,M),ANG(N,M),M=41,50),N=1,NE)
PRINT 608,(N,RAD(N,M),ANG(N,M),M=51,60),N=1,NE)
PRINT 608,(N,RAD(N,M),ANG(N,M),M=61,65),N=1,NE)
PRINT 1609,(N,RAD(N,M),ANG(N,M),M=61,65),N=1,NE)
PRINT 1603,(N,RAD(N,M),ANG(N,M),M=61,65),N=1,NE)
660 IF(LI)1630,1630,661
661 PRINT 670,(N,RAD(N,M),ANG(N,M),M=1,15),N=1,NE)
662 PRINT 604,(N,RAD(N,M),ANG(N,M),M=16,30),N=1,NE)
PRINT 605,(N,RAD(N,M),ANG(N,M),M=31,45),N=1,NE)
PRINT 604,(N,RAD(N,M),ANG(N,M),M=46,60),N=1,NE)
PRINT 604,(N,RAD(N,M),ANG(N,M),M=46,60),N=1,NE)

```



```

670 PRINT 1605,(N,N=61,65)
670 PRINT 1604,(N,(S(N,M),M=61,65),N=1,NE)
670 FORMAT(1H1,14X,22HCONCENTRATION AFTER T=,F9.0,/,8X,18,15I8//)
1609 FORMAT(//8X,17,6I8)
WRITING OF DATA FROM SELECTED POINTS ON TAPE
1638 LCP=LOP+10
1639 GO TO 614
1630 CONTINUE
640 DO 646 I=1,NURU
641 M=NZ(I)
642 N=MZ(I)
643 V2(I)=Z(N,M)
644 V3(I)=RAD(N,M)
645 V4(I)=ANG(N,M)
646 CONTINUE
647 WRITE(12) T,(V2(I),I=1,NURU)
WRITE(12) T,(V3(I),I=1,NURU)
WRITE(12) T,(V4(I),I=1,NURU)
602 FORMAT(1H1,14X,21HWATER HEIGHT AFTER T=,F9.0,9H SEC (CM),/8X,15I8/
1)
604 FORMAT(18,15F8.0//)
605 FORMAT(//8X,15I8//)
607 FORMAT(1H1,14X,76HRESULTANT CURRENT VELOCITY MAGNITUDE(CM/SEC) AND
1DIRECTION(DEGREES) AFTER T=,F9.0,4H SEC,/,8X,10I9)
606 FLRMAT((18,10(F4.0,1H,F4.0))//)
608 FLRMAT((18,10(F4.0,1H,F4.0))//)
1608 FLRMAT((18,5(F4.0,1H,F4.0))//)
609 FLRMAT(8X,17,9I9//)
1670 FLRMAT(//,5X,31HPOSITION OF DRIFTING OBJECT, N=,F6.2,2HM=,F6.2,//
1)
654 CONTINUE
3620 CONTINUE
RETURN
END
SUBROUTINE JOBS
COMMON HTZ,HTU,HTV,Z,U,V,US,VS,RAD,ANG,XK,YK,NU,MU,NK,MK,AH,CAPAP,
1PREC,ARG,P,PERU,NL,ML,NZ,MZ,V1,UPB,VPB,S,A,V2,V3,V4,HGU,HGV,H,
2B,AL,CAPA,CAPB,AINC,CAINC,NG,MG,TIT,AUS,TAR,OTC,T1,T2,T4,TE,TW,AI,
3A2,A3,A4,DT,BETA,ALPHA,F,R,DL,G,C3,NE,ME,NEH,MEH,JA,IUE,KKE,NURU
4,SI,T,RBETA,C1,SIGMA,ROL,A5,RU,RV,KO,LI,LE,LU,KI,LOP,IRB,TRE,TIC,
5LUN,LA,TIL,LIV,LEET,POSN,POSM,DRI,STV,ETV,TINCV,STH,ETC,TINCH,CNCU
6,CAINC
DIMENS1CN HTZ(24,65),HTU(24,65),HTV(24,65),Z(24,65),U(24,65),V(24,
165),US(24,65),VS(24,65),RAD(24,65),ANG(24,65),XK(24,65),YK(24,65),
2NU(6),MU(6),NK(10),MK(10),AH(7,10),CAPAP(7,10),PREC(7,10),ARG(7,10
3),PERU(5),NL(5),ML(5),NZ(20),MZ(20),V1(20),UPB(24,65),
4VPB(24,65),S(24,65),A(3),V2(20),V3(20),V4(20),HGU(24,65),HGV(24,65
5),H(7),B(7),AL(7),CAPA(7),CAPB(7),AINC(7),CAINC(7),NG(5),MG(5),

```



```

6 TIT(4), AUS(4), TAR(4), OTC(4)
  DIMENSION MAP(24,65), TITLE(8), UPLOT(24,65), VPLOT(24,65)
  OUTPUT OF SPECIAL POINTS
  REWIND 12
802 CCNTINUE
803 FORMAT(1H1,5X,114HWATER ELEVATION(CM) AND CURRENT VELOCITY RESULTS
  1 INT(MAGNITUDE IN CM(SEC AND DIRECTION IN DEGREES) AT SPECIAL POINTS
  2 //7X,4HTIME,4X,12(4X,A5)/15X,5(4X,A5)/)
804 FFORMAT(6X,5H(SEC),4X,12(2X,13,1H,,13)/15X,5(2X,13,1H,,13)//)
  OUTPUT AT SPECIAL POINTS
805 FORMAT(1H1,0,4X,12F9.2/15X,5F9.2)
806 FORMAT(5X,14HEND OF PROGRAM)
807 FFORMAT(15X,12(F4.0,1H,,F4.0)/15X,5(F4.0,1H,,F4.0)/)
808 PRINT 803,(V1(I),I=1,NURU)
809 PRINT 804,(V2(I),I=1,NURU)
810 READ(12) T,(V2(I),I=1,NURU)
  READ(12) T,(V3(I),I=1,NURU)
  READ(12) T,(V4(I),I=1,NURU)
813 PRINT 805,T,(V2(I),I=1,NURU)
814 PRINT 807,(V3(I),I=1,NURU)
815 IF (IE-T) 816,816,810
816 PRINT 806
  RETURN
  END

```

AMZ6690
 AMZ6700
 AMZ6710
 AMZ6720
 AMZ6730
 AMZ6740
 AMZ6750
 AMZ6760
 AMZ6770
 AMZ6780
 AMZ6790
 AMZ6800
 AMZ6810
 AMZ6820
 AMZ6830
 AMZ6840
 AMZ6850
 AMZ6860
 AMZ6870
 AMZ6880
 AMZ6890
 AMZ6900
 AMZ6910
 AMZ6920

BIBLIOGRAPHY

1. Defant, A., Physical Oceanography, v. 2, Pergamon Press, New York, N.Y., 1961.
2. Departamento Nacional da Producao Mineral, Divulgacao Tecnica No. 1, As Mais Recentes Medicoes do Rio Amazonas, by S. de Souza and others, Belem, PA, 1964.
3. Diegues, F.M.F., "Introducao a Oceanografia do Estuario Amazonico," Anais Hidrograficos, v. XXIX, P. 129-157, Rio de Janeiro, RJ, 1972.
4. Dronkers, J.J., Tidal Computations in Rivers and Coastal Waters, Wiley, New York, N.Y., 1964.
5. Department of Energy, Mines and Resources of Canada, Manuscript Report Series No. 17, Simulation of Tidal Motion in Complex River Systems and Inlets by a Method of Overlapping Segments, by R.F. Henry, 1971.
6. Environmental Prediction Research Facility Technical Paper No. 3-72, A Description of the EPRF Hydrodynamical-Numerical Model, by T. Laevastu and K. Rabe, March 1972.
7. Environmental Prediction Research Facility Technical Paper No. 1-74, A Vertically Integrated Hydrodynamical-Numerical Model (W. Hansen Type), by Oceanography Department of EPRF, January 1974.
8. Franco, A.S., Livro Texto de Mares para o Curso de Hidrografia para Oficiais, Directoria de Hidrografia do Ministerio da Marinha do Brasil, Rio de Janeiro, RJ, 1964.
9. Hansen, W., "Recent Development in Tidal Theory," Proceedings of the Symposium on Mathematical-Hydrodynamical Investigations of Physical Processes in the Sea - Moscow, May 1966, Hamburg, February 1968.
10. Hansen, W., "Theorie zur Errechnung des Wasserstandes und der Strömungen in Randmeeren nebst Anwendungen," Tellus, v. 8, p. 287-300, 1956.
11. Henderson, F.M., Open Channel Flow, MacMillan, New York, N.Y., 1967.
12. Gibbs, R.J., "Circulation in the Amazon River Estuary and Adjacent Atlantic Ocean," Journal of Marine Research, v. 28, p. 113-123, 1970.

13. Gibbs, R.J., "Amazon River Estuarine System," Geological Society of America Memoir No. 133, p. 85-88, 1972.
14. Ippen, A.T., Estuary and Coastline Hydrodynamics, McGraw-Hill, New York, N.Y., 1966.
15. Institute fur Meereskunde der Universitat Hamburg, Report No. 18-71, Hydrodynamical Numerical Investigations and Horizontal Dispersion of Seston in the River Elbe, by H.G. Ramming, February 1971.
16. Neuman, G., and Pierson, W.J., Principles of Physical Oceanography, Prentice Hall, Englewood Cliffs, N.J., 1966.
17. Ramming, H.G., "Shallow Water Tides," Proceedings of the Symposium on Mathematical-Hydrodynamical Investigations of Physical Processes in the Sea - Moscow, May 1966, Hamburg, February 1968.
18. Ramming, H.G., "Investigations of Motion Processes in Shallow Water Areas and Estuaries," Proceedings of the Symposium on Coastal Geodesy in Munich, p. 439-452, July 1970.
19. U.S. Geological Survey Circular 484, Amazon River Investigations, Reconnaissance Measurements of July 1963, by R.E. Oltman, H.O.R. Sternberg, F.C. Ames and L.C. Davis Jr., 1964.
20. U.S. Geological Survey Circular 552, Reconnaissance Investigations of the Discharge and Water Quality of the Amazon River, by R. Oltman, 1968.
21. Von Arx, W.S., An Introduction to Physical Oceanography, Addison Wesley, Reading, Ms, 1962.

INITIAL DISTRIBUTION LIST

	No. Copies
1. Defense Documentation Center Cameron Station Alexandria, Virginia 22314	2
2. Library, Code 0212 Naval Postgraduate School Monterey, California 93940	2
3. Department Chairman, Code 58 Department of Oceanography Naval Postgraduate School Monterey, California 93940	3
4. Dr. Stevens P. Tucker, Code 58 Tx (Thesis Advisor) Department of Oceanography Naval Postgraduate School Monterey, California 93940	4
5. CC. Luiz Antonio de Carvalho Ferraz Diretoria de Hidrografia e Navegacao Primeiro Distrito Naval Rio de Janeiro, RJ 20.000 Brazil	6
6. Diretor Diretoria de Hidrografia e Navegacao Primeiro Distrito Naval Rio de Janeiro, RJ 20.000 Brazil	3
7. Dr. Edward B. Thornton, Code 58 Tm Department of Oceanography Naval Postgraduate School Monterey, California 93940	1
8. Dr. Warren Thompson, Code 58 Th Department of Oceanography Naval Postgraduate School Monterey, California 93940	1
9. Dr. Taivo Laevastu Department of Oceanography Environmental Prediction Research Facility Naval Postgraduate School Monterey, California 939-0	2

10. Mr. Kevin Rabe 1
Department of Oceanography
Environmental Prediction Research Facility
Naval Postgraduate School
Monterey, California 93940
11. Office of Naval Research 1
Code 480
Arlington, Va 22217
12. Dr. Robert E. Stevenson 1
Scientific Liaison Office, ONR
Scripps Institution of Oceanography
La Jolla, Ca 92037
13. Petroleo Brasileiro SA 1
Centro de Pesquisas e Desenvolvimento
Rio de Janeiro, RJ 20.000 Brazil
14. Diretor 2
Instituto Oceanografico
Universidade de Sao Paulo
Alameda Eduardo Prado 698
Sao Paulo, SP 01000, Brazil
15. Diretor 2
Segundo Distrito da Divisao de Aguas
Belem do Para, PA, 66.000 Brazil
16. Diretor 1
Divisao do Porto de Santana
Industria e Comercio de Minerios (ICOMI)
Macapa, Amapa - Brazil
17. Dr. Walther Hansen 1
Attn. Institut fur Meereskunde
Universitat Hamburg
Hamburg, Germany
18. Oceanographer of the Navy 1
Hoffman Building No. 2
200 Stovall Street
Alexandria, Va 22332
19. U.S. Geological Survey 1
Attn. Library
Washington, DC 20390
20. Library, Code 3330 1
Naval Oceanographic Office
Washington, DC 20373

- | | | |
|-----|--|---|
| 21. | SIO Library
University of California, San Diego
P.O. Box 2367
La Jolla, Ca 92037 | 1 |
| 22. | Department of Oceanography Library
University of Washington
Seattle, Wa 98105 | 1 |
| 23. | Department of Oceanography Library
Oregon State University
Corvallis, Oregon 97331 | 1 |
| 24. | Commanding Officer
Fleet Numerical Weather Central
Monterey, Ca 93940 | 1 |
| 25. | Commanding Officer
Environmental Prediction Research Facility
Monterey, Ca 93940 | 1 |
| 26. | Department of the Navy
Commander, Oceanographic System Pacific
Box 1390
FPO San Francisco 96610 | 1 |



162806

Thesis

F2645 Ferraz

c.1

Tidal and current
prediction for the
Amazon's North Chan-
nel using a hydrody-
namical-numerical model.

162806

Thesis

F2645 Ferraz

c.1

Tidal and current
prediction for the
Amazon's North Chan-
nel using a hydrody-
namical-numerical model.

thesF2645

Tidal and current prediction for the Ama



3 2768 002 06557 5

DUDLEY KNOX LIBRARY